Analytical theory of neutrino oscillations in matter with *CP* violation

Mikkel B. Johnson

Los Alamos National Laboratory, Los Alamos, New Mexico 87545, USA

Ernest M. Henley

Department of Physics, University of Washington, Seattle, Washington 98195, USA

Leonard S. Kisslinger

Department of Physics, Carnegie-Mellon University, Pittsburgh, Pennsylvania 15213, USA

We develop an exact analytical formulation of neutrino oscillations in matter within the framework of the standard neutrino model assuming three Dirac neutrinos. Our Hamiltonian formulation, which includes *CP* violation, leads to expressions for the partial oscillation probabilities that are linear combinations of spherical Bessel functions in the eigenvalue differences. The coefficients of these Bessel functions are polynomials in the neutrino CKM matrix elements, the neutrino mass differences squared, the strength of the neutrino interaction with matter, and the neutrino mass eigenvalues in matter. We give exact closed-form expressions for all partial oscillation probabilities in terms of these basic quantities. Adopting the standard neutrino model, we then examine how the exact expressions for the partial oscillation probabilities might simplify by expanding in one of the small parameters α and $\sin\theta_{13}$ of this model. We show explicitly that for small α and $\sin\theta_{13}$, there are branch points in the analytic structure of the eigenvalues that lead to singular behavior of expansions near the solar and atmospheric resonances. We present numerical calculations that indicate how to use the small-parameter expansions in practice.

I. INTRODUCTION

In this paper, we develop an exact analytical representation of neutrino oscillations [1] in matter within the framework of the standard neutrino model (SNM) [2] with three Dirac neutrinos. The exact closed-form expressions we give for the time-evolution operator $S(t, t')$ are obtained from H_ν using the Lagrange interpolation formula given in Ref. [3]. The resulting expressions are easily evaluated without any approximations.

The paper is divided into two main parts. In the first, we summarize the main results of our theory. Details underlying the derivation are given in Appendixes. We also retrieve the well-known two-neutrino flavor results as a special case of our general results.

In the second part we address other analytical formulations found in the literature. The expansion of the neutrino oscillation probability in one of the small parameters α and $\sin^2\theta_{13}$ of the SNM for H_ν is of particular interest. The seminal work along these lines is found in Refs. [4–6]. This work underlies many of the analyses and exploratory studies of experiments at present and future neutrino facilities, including our earlier work [7–10].

The present paper was undertaken, and used, for the purpose of independently confirming the results of Refs. [7–10]. We find that the accuracy of the expanded oscillation probability is restricted by the presence of branch points in the analytic structure of the eigenvalues

of neutrinos propagating in matter. We also show that the regions where the expanded results are reliable is different for expansions in α [4] and $\sin^2\theta_{13}$ [5,6]. We then map out regions where the expanded results are reliable by comparing numerical results to the exact results of our Hamiltonian formulation.

Another recent study [11] takes a complementary approach and finds that the predictions of Refs. [7–10] can be improved in certain regions using an exact evaluation of the integral $I_{\alpha*}$ rather than the approximate one found there. It concludes that within these regions, predictions of (μ, e) oscillations improve for certain values of the experimental parameters.

The dimensionalities of the neutrino Hamiltonian H_ν and the parameter space characterizing the mixing of three neutrino pairs are sources of difficulty for finding a tractable representation of the oscillation probability. The Lagrange interpolation formula [3] is enormously helpful, providing an exact and formally elegant expression for the exponentiation of an $n \times n$ matrix.

The description of two-flavor neutrino oscillations is elementary by comparison. In that case, H_ν is a 2×2 matrix, and the mixing is described by a single real parameter.

II. NEUTRINO DYNAMICS

We will be interested in the dynamics of the three known neutrinos and their corresponding antineutrinos in matter.

This dynamics is determined by the time-dependent Schrödinger equation,

$$i\frac{d}{dt}|\nu(t)\rangle = H_\nu|\nu(t)\rangle, \tag{1}$$

where the neutrino Hamiltonian,

$$H_\nu = H_{0v} + H_1, \tag{2}$$

consists of a piece H_{0v} describing neutrinos in the vacuum and a piece H_1 describing their interaction with matter.

The solutions of Eq. (1) may be expressed in terms of stationary-state solutions of the eigenvalue (EV) equation

$$H_\nu|\nu_{mi}\rangle = E_i|\nu_{mi}\rangle, \tag{3}$$

where the label "m" indicates neutrino mass eigenstates, as distinguished from their flavor states sometimes denoted with the label "f." In operator form, this dynamics may be expressed in terms of the time-evolution operator $S(t',t)$, which describes completely the evolution of states from time t to t' and also satisfies the time-dependent Schrödinger equation.

We will examine neutrinos propagating in a uniform medium for interactions constant not only in space but also time. Because the Hamiltonian is then translationally invariant, attention may be restricted to states, both in the vacuum and in matter, characterized by momentum $\vec{p}$ and, therefore, having the overall r dependence $e^{i\vec{p}\cdot\vec{r}}$. In this case expressions may be simplified by suppressing the overall plane wave, a convention we adopt.

For time-independent interactions, $S(t',t)$,

$$S(t',t) = e^{-iH_\nu(t'-t)}, \tag{4}$$

depends on time only through the time *difference* $t' - t$. Then, written in terms of the stationary state solutions $|\nu_{mi}\rangle$ of Eq. (1),

$$S(t',t) = \sum_i |\nu_{mi}\rangle e^{-iE_i(t'-t)}\langle\nu_{mi}|. \tag{5}$$

With the momentum dependence factored out, three basis states $|M(i)\rangle, i = (1,2,3)$ are then required to describe three neutrinos. The basis states correspond to a specific representation, as in descriptions of a spin-1 object. The basis should, of course, be orthogonal,

$$\langle M(i)|M(j)\rangle = \delta_{ij}, \tag{6}$$

and complete,

$$\sum_k |M(k)\rangle\langle M(k)| = \mathbf{1}. \tag{7}$$

Once the basis is chosen, wave functions for a neutrino state are naturally introduced as the components of this

state in the chosen basis. For example, with the eigenstates of Eq. (3) expanded in the basis,

$$|\nu_{mj}\rangle = \sum_i |M(i)\rangle m_j^i, \tag{8}$$

the wave functions of $|\nu_{mj}\rangle$ would be the set $m_j^i, i = (1,2,3)$. With the plane wave factored out, the wave function is just a set of three numbers. Additionally, introduction of a basis makes it possible to represent neutrino states and operators such as H_ν in matrix form, with each entry in the matrix corresponding to a projection of the object being described onto the basis.

In this paper we take the Hamiltonian in Eq. (2) to be expressed in the *standard representation*, where the mass basis states $|M(i)\rangle$ are taken as the set of states that diagonalize the neutrino vacuum Hamiltonian H_{0v}, i.e., $|M(i)\rangle \equiv |\nu_{mi}^0\rangle = |\bar{\nu}_{mi}^0\rangle$,

$$H_{0v}|\nu_{mi}^0\rangle = E_i^0|\nu_{mi}^0\rangle. \tag{9}$$

In matrix form

$$H_{0v} = \begin{pmatrix} E_3^0 & 0 & 0 \\ 0 & E_2^0 & 0 \\ 0 & 0 & E_1^0 \end{pmatrix}, \tag{10}$$

with the EVs taken to be ordered $E_1^0 \leq E_2^0 \leq E_3^0$ as in the normal mass hierarchy. In the literature, the Hamiltonian is often expressed in a different basis obtained by rotating to one in which the complete neutrino Hamiltonian is diagonal as in Ref. [4].

We assume here that neutrinos and antineutrinos represented by $|\nu_{mi}^0\rangle$ and $|\bar{\nu}_{mi}^0\rangle$, respectively, are the structureless elementary Dirac fields of the standard neutrino model [2]. For this reason the theory is invariant under *CPT*, so the mass of an antineutrino in the vacuum is the same as that for its corresponding neutrino.

A. Flavor and mass states

Neutrinos are produced and detected in states of good flavor, $|\nu_{fi}\rangle$. The three flavors, electron (e), muon (μ), and tau (τ) correspond, respectively, to the index values $i = (1,2,3)$. In the vacuum, each flavor state is a specific linear combination of the three mass eigenstates $|M(i)\rangle$ of the neutrino vacuum Hamiltonian H_{0v}. This linear combination is expressed in terms of the same set of numbers U_{ij} for both neutrinos and antineutrinos

$$|\nu_{fi}^0\rangle = \sum_j U_{ij}^*|M(j)\rangle$$

$$|\bar{\nu}_{fi}^0\rangle = \sum_j U_{ij}|M(j)\rangle, \tag{11}$$

where U_{ij} are the elements of a unitary operator U, the neutrino analog of the familiar CKM matrix. It is standard to express U_{ij} in terms of three mixing angles $(\theta_{12}, \theta_{13}, \theta_{23})$ and a phase δ_{cp} characterizing CP violation,

$$
\begin{pmatrix}
c_{12}c_{13} & s_{12}c_{13} & s_{13}e^{-i\delta_{cp}} \\
U_{21} & U_{22} & s_{23}c_{13} \\
U_{31} & U_{32} & c_{23}c_{13}
\end{pmatrix},
\tag{12}
$$

where

$$
\begin{aligned}
U_{21} &= -s_{12}c_{23} - c_{12}s_{23}s_{13}e^{i\delta_{cp}} \\
U_{22} &= c_{12}c_{23} - s_{12}s_{23}s_{13}e^{i\delta_{cp}} \\
U_{31} &= s_{12}s_{23} - c_{12}c_{23}s_{13}e^{i\delta_{cp}} \\
U_{32} &= -c_{12}s_{23} - s_{12}c_{23}s_{13}e^{i\delta_{cp}}.
\end{aligned}
\tag{13}
$$

We use here the standard abbreviation $s_{12} \equiv \sin\theta_{12}$, $c_{12} \equiv \cos\theta_{12}$, *etc.* The parameters θ and δ_{cp} are determined from experiment.

Because $U_{ij} \to U_{ij}^*$ with $\delta_{cp} \to -\delta_{cp}$ it follows that the relationship in Eq. (11) between flavor and mass states for antineutrinos and neutrinos in the vacuum is equivalent to $\delta_{cp} \leftrightarrow -\delta_{cp}$.

B. Neutrino interacting Hamiltonian

The interaction H_1, determined by taking the electron flavor states scattering from the electrons of the medium to mediate the interaction, is then expressed as an operator in the standard representation,

$$
H_1 = U^{-1}
\begin{pmatrix}
V & 0 & 0 \\
0 & 0 & 0 \\
0 & 0 & 0
\end{pmatrix}
U,
\tag{14}
$$

with $V = \pm\sqrt{2}G_F n_e$ and n_e the electron number density in matter. For electrically neutral matter consisting of protons, neutrons, and electrons, the electron density n_e is the same as the proton density n_p,

$$
\begin{aligned}
n_e &= n_p \\
&= \frac{n_n}{R},
\end{aligned}
\tag{15}
$$

where n_n is the average total nucleon number density and R is the average proton-neutron ratio. In the Earth's mantle, the dominant constituents of matter are the light elements, so $R \approx 1/2$; in the surface of a neutron star $R \ll 1$. Matrix elements of H_1 are, thus,

$$
\langle M(k)|H_1|M(k')\rangle = U_{1k}^* V U_{1k'}.
\tag{16}
$$

C. Dimensionless variables

The results are most naturally expressed in dimensionless variables. We first take advantage of the global phase invariance to express all energies relative to the vacuum EV E_1^0 of the same momentum. We indicate that a quantity is expressed relative to E_1^0 by placing a bar over it, e.g.,

$$
\bar{E}_i^0 \equiv E_i^0 - E_1^0.
\tag{17}
$$

We follow the same convention for the Hamiltonian,

$$
\bar{H}_\nu \equiv H_\nu - \mathbf{1}E_1^0,
\tag{18}
$$

so the EV equation Eq. (3) becomes

$$
(\bar{H}_{0v} + H_1)|\nu_{mi}\rangle = \bar{E}_i|\nu_{mi}\rangle,
\tag{19}
$$

where

$$
\bar{H}_{0v} \equiv H_{0v} - \mathbf{1}E_1^0.
\tag{20}
$$

Then, to express the theory in dimensionless variables we divide all energies, including the Hamiltonian, by $\bar{E}_3^0 = E_3^0 - E_1^0$. The stationary-states $|\nu_{mi}\rangle$ are also be determined from the dimensionless Hamiltonian $\hat{\bar{H}}_\nu$,

$$
\hat{\bar{H}}_\nu = \hat{\bar{H}}_{0v} + \hat{H}_1,
\tag{21}
$$

i.e., from the solutions of

$$
\hat{\bar{H}}_\nu|\nu_{mi}\rangle = \hat{\bar{E}}_i|\nu_{mi}\rangle,
\tag{22}
$$

where the "hat" placed over a quantity indicates it is dimensionless. Thus,

$$
\begin{aligned}
\hat{\bar{E}}_i &\equiv \frac{\bar{E}_i}{\bar{E}_3^0} \\
\hat{\bar{H}}_{0v} &\equiv \frac{\bar{H}_{0v}}{\bar{E}_3^0},
\end{aligned}
\tag{23}
$$

and $\hat{H}_1$ is obtained from H_1 by replacing

$$
V \to \hat{A} \equiv \frac{V}{\bar{E}_3^0}.
\tag{24}
$$

The quantity $\hat{A}$ is the same as that defined in Refs. [4,7–11]. The connection of the Hamiltonian $\hat{\bar{H}}_\nu$ to the full Hamiltonian $H_\nu = H_{0v} + H_1$ is then

$$
H_\nu = \mathbf{1}E_1^0 + \bar{E}_3^0\hat{\bar{H}}_\nu.
\tag{25}
$$

D. Neutrino vacuum Hamiltonian $\hat{\bar{H}}_{0v}$

The case of main interest for many situations is the ultrarelativistic limit, $|p| \gg m^2$ (we take the speed

of light $c = 1$). For ultrarelativistic neutrinos in the laboratory frame, the energy of a neutrino in the vacuum becomes

$$E_i^0 \approx |\vec{p}| + \frac{m_i^2}{2E}, \tag{26}$$

where m_i is its mass the vacuum. Similarly, E_i appearing in Eq. (3) may be written

$$E_i \approx |\vec{p}| + \frac{M_i^2}{2E}, \tag{27}$$

where M_i is its mass in the medium. Thus, in this limit,

$$\hat{\hat{E}}_i \rightarrow \frac{M_i^2 - m_1^2}{m_3^2 - m_1^2} \tag{28}$$

and

$$\hat{\hat{H}}_{0v} \rightarrow \begin{pmatrix} 0 & 0 & 0 \\ 0 & \alpha & 0 \\ 0 & 0 & 1 \end{pmatrix} \tag{29}$$

with

$$\alpha \equiv \frac{m_2^2 - m_1^2}{m_3^2 - m_1^2}. \tag{30}$$

In this limit, the distance L from the source to the detector corresponding to $S(t', t)$ in Eq. (4) is

$$L = t' - t. \tag{31}$$

The time-evolution operator, Eq. (4), expressed in dimensionless variables is

$$\begin{aligned} S(L) &= e^{-iH_v(t'-t)} \\ &= e^{2i\hat{\hat{E}}_1^0 \Delta_L} e^{-2i\hat{\hat{H}}_v \Delta_L}, \end{aligned} \tag{32}$$

where $\hat{\hat{H}}_v$ is given in Eq. (25), and where

$$\Delta_L \equiv \frac{L(m_3^2 - m_1^2)}{4E}. \tag{33}$$

[The similar quantity Δ_L as defined in Ref. [7] is exactly one-half of that appearing in Eq. (33).]

E. Neutrino mass eigenvalues

The neutrino mass eigenstates in a medium are solutions to the EV equation for $\hat{\hat{H}}_v$, Eq. (22). In many familiar formulations [4–6] the full solutions, including both the eigenstates $|\nu_i\rangle$ and EVs $\hat{\hat{E}}_i$, are required to find the neutrino oscillation probabilities.

1. Diagonalization of neutrino Hamiltonian

The energies $\hat{\hat{E}}_i$ are solutions of the cubic equation [12]

$$\hat{\hat{E}}_i^{\,3} + a\hat{\hat{E}}_i^{\,2} + b\hat{\hat{E}}_i + c = 0, \tag{34}$$

where

$$\begin{aligned} a &= -(1 + \alpha + \hat{A}) \\ b &= \alpha + \hat{A}\cos^2\theta_{13} + \hat{A}\alpha C_2^{(+)} \\ c &= -\hat{A}\alpha\cos^2\theta_{12}\cos^2\theta_{13}. \end{aligned} \tag{35}$$

We have expressed b in terms of a frequently recurring combination of mixing angles,

$$C_2^{(\pm)} \equiv \cos^2\theta_{12} \pm \sin^2\theta_{12}\sin^2\theta_{13}. \tag{36}$$

Note that the mass eigenstate energies are independent of δ_{cp} and θ_{23} for both neutrinos and antineutrinos.

The solutions of Eq. (34) are expressed conveniently in terms of the quantity d,

$$\begin{aligned} d &= \psi + \sqrt{\psi^2 - 4\gamma^3} \\ \gamma &\equiv a^2 - 3b \\ \psi &\equiv a^3 - 27c - 3a\gamma. \end{aligned} \tag{37}$$

These solutions are real when

$$|d^{1/3}|^2 = 2^{2/3}\gamma > 0, \tag{38}$$

which requires

$$\psi^2 < 4\gamma^3, \tag{39}$$

and, thus, that d be complex. Because having real energies is required by Hermiticity of the neutrino Hamiltonian, Eqs. (38) and (39) amount to conditions on all parameter sets in terms of which H_v is defined.

We find

$$\begin{aligned} \hat{\hat{E}}_1 &= -\frac{a}{3} - \frac{1}{3 \cdot 2^{1/3}}\left(\sqrt{3}\,\text{Im}[d^{1/3}] + \text{Re}[d^{1/3}]\right) \\ \hat{\hat{E}}_2 &= -\frac{a}{3} + \frac{1}{3 \cdot 2^{1/3}}\left(\sqrt{3}\,\text{Im}[d^{1/3}] - \text{Re}[d^{1/3}]\right) \\ \hat{\hat{E}}_3 &= -\frac{a}{3} + \frac{2^{2/3}}{3}\,\text{Re}[d^{1/3}]. \end{aligned} \tag{40}$$

The masses are ordered so that $m_3 > m_2 > m_1$. Because EV do not cross, $\hat{\hat{E}}_3 > \hat{\hat{E}}_2 > \hat{\hat{E}}_1$ for all $|\hat{A}|$. A simple constraint among $\hat{\hat{E}}_i$ is found from the trace of Eq. (21),

$$\mathrm{Tr}\hat{\hat{H}}_\nu = \hat{\hat{E}}_1 + \hat{\hat{E}}_2 + \hat{\hat{E}}_3$$
$$= \mathrm{Tr}\hat{\hat{H}}_{0v} + \mathrm{Tr}\hat{H}_1$$
$$= 1 + \alpha + \hat{A} \equiv -a. \qquad (41)$$

2. Using neutrino mass eigenvalues in our Hamiltonian formulation

In our formulation, the entire dependence of the time evolution operator on the neutrino eigenvalues occurs through three eigenvalue combinations,

$$\Delta\hat{\hat{E}}_{\ell\ell'} \equiv \hat{\hat{E}}_\ell - \hat{\hat{E}}_{\ell'}$$
$$\Sigma_{\ell\ell'} \equiv \hat{\hat{E}}_\ell + \hat{\hat{E}}_{\ell'}$$
$$\Pi_{\ell\ell'} \equiv \hat{\hat{E}}_\ell\hat{\hat{E}}_{\ell'}, \qquad (42)$$

with $\ell > \ell'$ (and powers thereof). We denote such quantities using a bracket notation. For example,

$$\Delta\hat{\hat{E}}[1] = \hat{\hat{E}}_3 - \hat{\hat{E}}_2$$
$$\Delta\hat{\hat{E}}[2] = \hat{\hat{E}}_3 - \hat{\hat{E}}_1$$
$$\Delta\hat{\hat{E}}[3] = \hat{\hat{E}}_2 - \hat{\hat{E}}_1, \qquad (43)$$

in the case of $\Delta\hat{\hat{E}}$. We will generally use this bracket notation also for other quantities in our formulation that depend on two indices (ℓ, ℓ'), such as $\Sigma_{\ell\ell'}$ and $\Pi_{\ell\ell'}$.

An expression for $\Sigma[\ell]$,

$$\Sigma[\ell] = -a - \hat{\hat{E}}_\ell, \qquad (44)$$

follows from Eq. (41). An equivalent expression for $\Pi[\ell]$ in terms of $\hat{\hat{E}}_\ell$ is found by subtracting Eq. (34) for $\hat{\hat{E}}_\ell$ and that for $\hat{\hat{E}}_{\ell'}$ and dividing through by $\Delta\hat{\hat{E}}_{\ell\ell'}$. We find

$$0 = (\hat{\hat{E}}_\ell^2 + \hat{\hat{E}}_\ell\hat{\hat{E}}_{\ell'} + \hat{\hat{E}}_{\ell'}^2) + a(\hat{\hat{E}}_\ell + \hat{\hat{E}}_{\ell'}) + b$$
$$= (\hat{\hat{E}}_\ell + \hat{\hat{E}}_{\ell'})^2 - \hat{\hat{E}}_\ell\hat{\hat{E}}_{\ell'} + a(\hat{\hat{E}}_\ell + \hat{\hat{E}}_{\ell'}) + b, \qquad (45)$$

giving

$$\Sigma[\ell]^2 - \Pi[\ell] + a\Sigma[\ell] + b = 0. \qquad (46)$$

Then, using Eq. (44),

$$\Pi[\ell] = \Sigma_\ell(\Sigma_\ell + a) + b$$
$$= b + a\hat{\hat{E}}_\ell + \hat{\hat{E}}_\ell^2. \qquad (47)$$

Finally, having observed that powers of the quantities given in Eq. (42) will appear in various expressions, we note that $\Pi[\ell]^p$ and $\Sigma[\ell]^q$ with $p \geq 2$ and $q \geq 3$ involve linear combinations of eigenvalues $\hat{\hat{E}}_\ell^n$ with powers $n \geq 3$.

Such terms are equivalently represented by a linear combination of three terms, one proportional to $\hat{\hat{E}}_\ell^2$, one proportional to $\hat{\hat{E}}_\ell$, and one independent of $\hat{\hat{E}}_\ell$, obtained by using the equation of motion repeatedly. We later make use of this fact to simplify various expressions.

III. THE S-MATRIX IN OUR HAMILTONIAN FORMULATION

The probability $\mathcal{P}(\nu_a \rightarrow \nu_b)$ for neutrinos to oscillate from the initial state of flavor a to a final state of flavor b is found from the time-evolution operator $S(t', t)$ as

$$\mathcal{P}(\nu_a \rightarrow \nu_b) = |S^{ab}(t', t)|^2$$
$$\equiv P^{ab}(t' - t), \qquad (48)$$

where

$$|S^{ab}(t', t)|^2 = |\langle\nu_{fb}^0|S(t', t)|\nu_{fa}^0\rangle|^2. \qquad (49)$$

We accordingly determine here $P^{ab}(t' - t)$ from $S(t', t)$ defined in Eq. (4).

In this section we review the formulation of neutrino oscillations based on the Lagrange interpolation formula as used in Ref. [3]. This formulation leads to exact, closed-form expressions for the time-evolution operator and the partial oscillation probabilities that are linear combinations of spherical Bessel functions in the eigenvalue differences whose coefficients are polynomials in the neutrino CKM matrix elements, the neutrino mass differences squared, the strength of the neutrino interaction with matter, and the neutrino mass eigenvalues in matter. We are led quite naturally to such expressions for all the partial oscillation probabilities in terms of these basic quantities. The numerical results given later in this paper are based on this formulation.

A. Time-evolution operator

The overall phase in Eq. (32) does not contribute to $|S^{ab}(t', t)|^2$, so for the purpose of calculating the oscillation probability, we may take

$$S(L) \rightarrow e^{-i\hat{\hat{H}}_\nu\Delta_L}. \qquad (50)$$

Then, with neutrinos created and detected in flavor states, which are coherent linear combinations of the neutrino vacuum mass eigenstates given in Eq. (9),

$$|\nu_{fa}^0\rangle = \sum_j U_{aj}^*|M(j)\rangle, \qquad (51)$$

we see that the mass eigenstate components of the flavor states contribute coherently to the time-evolution operator. Thus,

$$\langle \nu_{fb}^0 | e^{-i\hat{H}_\nu \Delta_L} | \nu_{fa}^0 \rangle = \langle M(b) | U e^{-i\hat{H}_\nu \Delta_L} U^\dagger | M(a) \rangle. \quad (52)$$

This coherence leads to the oscillation phenomenon.

The elegant formulas for $S(L) \equiv e^{-i\hat{H}_\nu \Delta_L}$ are obtained from the Lagrange interpolation formula, Eqs. (9) and (11) of Ref. [3],

$$U e^{-i\hat{H}_\nu \Delta_L} U^{-1} = \sum_\ell F_\ell \exp^{-i\hat{E}_\ell \Delta_L}, \quad (53)$$

where $T = L = t' - t$ and

$$F_\ell \equiv \Pi_{j \neq \ell} \frac{U \hat{H}_\nu U^{-1} - \mathbf{1}\hat{E}_j}{\hat{E}_\ell - \hat{E}_j}. \quad (54)$$

For three neutrinos, the sum in Eq. (106) runs over three values of ℓ and the product in Eq. (54) over two values of j.

Using the convention that O^{ab}, written without parentheses enclosing ab, denotes the matrix elements of the operator O,

$$O^{ab} \equiv \langle M(b) | O | M(a) \rangle, \quad (55)$$

the matrix elements F_ℓ^{ab} of F_ℓ given in Eq. (54) may be compactly written

$$F_\ell^{ab} = \frac{\langle M(b) | \hat{W}[\ell] | M(a) \rangle}{\hat{D}[\ell]}, \quad (56)$$

where [3],

$$\hat{W}[1] \equiv (U \hat{H}_\nu U^{-1} - \mathbf{1}\hat{E}_3)(U \hat{H}_\nu U^{-1} - \mathbf{1}\hat{E}_2)$$
$$\hat{W}[2] \equiv (U \hat{H}_\nu U^{-1} - \mathbf{1}\hat{E}_3)(U \hat{H}_\nu U^\dagger - \mathbf{1}\hat{E}_1)$$
$$\hat{W}[3] \equiv (U \hat{H}_\nu U^{-1} - \mathbf{1}\hat{E}_2)(U \hat{H}_\nu U^\dagger - \mathbf{1}\hat{E}_1) \quad (57)$$

and

$$\hat{D}[1] = (\hat{E}_3 - \hat{E}_1)(\hat{E}_2 - \hat{E}_1)$$
$$\hat{D}[2] = (\hat{E}_1 - \hat{E}_2)(\hat{E}_3 - \hat{E}_2)$$
$$\hat{D}[3] = (\hat{E}_1 - \hat{E}_3)(\hat{E}_2 - \hat{E}_3). \quad (58)$$

Equations (57), (58) use the same bracket notation introduced in Eq. (33). The result in Eqs. (52), (106), and (54) is immediately verified to be correct by inserting a complete set of intermediate eigenstates of H_ν in Eq. (57).

It follows from the unitarity of U that $\hat{W}[\ell]$ is Hermitian,

$$\hat{W}[\ell]^\dagger = \hat{W}[\ell] \quad (59)$$

and that the two factors in Eqs. (57) commute with each other. We find from Eq. (57) that

$$\mathrm{Tr}\hat{W}[\ell] = \hat{D}[\ell]. \quad (60)$$

Equation (59) establishes the reflection symmetry,

$$F_\ell^{ab*} = F_\ell^{ba}. \quad (61)$$

Explicit expressions for $\hat{W}[\ell]$ are easily found in terms of H_ν. The entire dependence of $\hat{W}[\ell]$ on δ_{cp} occurs through three operators independent of δ_{cp}, $W_0[\ell]$, $W_{\cos}[\ell]$ and $W_{\sin}[\ell]$,

$$\hat{W}[\ell] = \hat{W}_0[\ell] + \cos\delta_{cp}\hat{W}_{\cos}[\ell]$$
$$+ i\sin\delta_{cp}\hat{W}_{\sin}[\ell], \quad (62)$$

with $\hat{W}_0[\ell]$, $\hat{W}_{\cos}[\ell]$ and $\hat{W}_{\sin}[\ell]$ real and independent of δ_{cp}. Details are given in Appendix A.

B. Total oscillation probability

Expressions for $\mathcal{P}(\nu_a \to \nu_b)$ may be obtained directly from $S(L)$,

$$\mathcal{P}(\nu_a \to \nu_b) = |S^{ab}(t', t)|^2$$
$$= \mathrm{Re}[S^{ab}(L)]^2 + \mathrm{Im}[S^{ab}(L)]^2. \quad (63)$$

Convenient expressions for $\mathrm{Re}[S^{ab}(L)]$ and $\mathrm{Im}[S^{ab}(L)]$ defined by Eq. (106) are presented in Appendix A. In our Hamiltonian formulation, the dependence of $S(T)$ on the CP violating phase δ_{cp} is very simple and follows from Eqs. (106) and (62) noting that $F_\ell^{ab} = \hat{W}^{ab}[\ell]/\hat{D}[\ell]$, Eq. (56). We, thus, find

$$\mathrm{Re}[S^{ab}(t', t)] = \delta_{ab} - 2\sum_\ell \frac{\hat{W}_0^{ab}[\ell]}{\hat{D}[\ell]} \sin^2 \hat{E}_\ell \Delta_L$$
$$- 2\cos\delta_{cp}\sum_\ell \frac{\hat{W}_{\cos}^{ab}[\ell]}{\hat{D}[\ell]} \sin^2 \hat{E}_\ell \Delta_L$$
$$+ \sin\delta_{cp}\sum_\ell \frac{\hat{W}_{\sin}^{ab}[\ell]}{\hat{D}[\ell]} \sin 2\hat{E}_\ell \Delta_L, \quad (64)$$

and

$$\mathrm{Im}[S^{ab}(t', t)] = -2\sin\delta_{cp}\sum_\ell \frac{\hat{W}_{\sin}^{ab}[\ell]}{\hat{D}[\ell]} \sin^2 \hat{E}_\ell \Delta_L$$
$$- \sum_\ell \frac{\hat{W}_0^{ab}[\ell]}{\hat{D}[\ell]} \sin 2\hat{E}_\ell \Delta_L$$
$$- \cos\delta_{cp}\sum_\ell \frac{\hat{W}_{\cos}^{ab}[\ell]}{\hat{D}[\ell]} \sin 2\hat{E}_\ell \Delta_L, \quad (65)$$

where Δ_L is defined in Eq. (33). Approximate expressions for $\mathcal{P}(\nu_a \to \nu_b)$ in terms of the parameters of H_ν were obtained from $S(L)$ in Refs. [5,6] by an expansion in $\sin\theta_{13}$.

C. Partial oscillation probabilities

Using somewhat different techniques, the oscillation probability may be expressed through a set of functions that express how $\mathcal{P}(\nu_a \to \nu_b) \equiv P^{ab}$ depends on the CP violating phase δ_{cp} [4]. In our Hamiltonian formulation there are four such terms,

$$P^{ab} = \delta(a,b) + P^{ab}_0 + P^{ab}_{\sin\delta} + P^{ab}_{\cos\delta} + P^{ab}_{\cos^2\delta}, \quad (66)$$

with $P^{ab}_{\sin\delta}$ linear in $\sin\delta_{cp}$, $P^{ab}_{\cos\delta}$ linear in $\cos\delta_{cp}$, $P^{ab}_{\cos^2\delta}$ quadratic in $\cos\delta_{cp}$, and P^{ab}_0 independent of δ_{cp}. Although only the overall oscillation probability is a true probability, guaranteed to be strictly positive everywhere, we find it convenient to refer to these four terms as "partial oscillation probabilities." Approximate expressions for the partial oscillation probabilities expanded in the small parameter α of the SNM in Ref. [4].

Obtaining expressions for the partial oscillation probabilities from the time-evolution operator requires additional analysis, given in Appendix B. In terms of spherical Bessel functions, we find there

$$P^{ab}_{\sin\delta}(\Delta_L, \hat{A}) = \sin\delta_{cp} \frac{4\Delta_L}{\hat{D}} \sum_\ell (-1)^\ell w^{ab}_{\sin}[\ell] j_0(2\hat{\Delta}[\ell]),$$

$$(67)$$

where $w^{ab}_{\sin}[\ell]$ and, therefore, $P^{ab}_{\sin\delta}$ are antisymmetric under $a \leftrightarrow b$. The other three partial oscillation probabilities are individually symmetric under $a \leftrightarrow b$. We find

$$P^{ab}_{\cos\delta}(\Delta_L, \hat{A}) = -\cos\delta_{cp} \frac{4\Delta_L^2}{\hat{\hat{D}}} \sum_\ell (-1)^\ell w^{ab}_{\cos}[\ell]$$
$$\times \Delta\hat{\hat{E}}[\ell] j_0^2(\hat{\Delta}[\ell])$$

$$P^{ab}_{\cos^2\delta}(\Delta_L, \hat{A}) = -\cos^2\delta_{cp} \frac{4\Delta_L^2}{\hat{D}} \sum_\ell (-1)^\ell w^{ab}_{\cos^2}[\ell]$$
$$\times \Delta\hat{\hat{E}}[\ell] j_0^2(\hat{\Delta}[\ell])$$

$$P^{ab}_0(\Delta_L, \hat{A}) = -\frac{4\Delta_L^2}{\hat{D}} \sum_\ell (-1)^\ell w^{ab}_0[\ell] \Delta\hat{\hat{E}}[\ell] j_0^2(\hat{\Delta}[\ell]),$$

$$(68)$$

where all sums run over $\ell = 1, 2, 3$, $\hat{\Delta}[\ell]$ is defined as

$$\hat{\Delta}[\ell] \equiv \Delta\hat{\hat{E}}[\ell]\Delta_L, \quad (69)$$

with $\Delta\hat{\hat{E}}[\ell]$ defined in Eq. (43), $\hat{D}$ is defined as

$$\hat{D} \equiv \Delta\hat{\hat{E}}[1]\Delta\hat{\hat{E}}[2]\Delta\hat{\hat{E}}[3], \quad (70)$$

and the matrix elements $w^{ab}_i[\ell]$ are given in terms of the mixing angles and $\hat{A}$ in Appendix B. Since we order the energies so that $\hat{\hat{E}}_3 > \hat{\hat{E}}_2 > \hat{\hat{E}}_1$, $\Delta\hat{\hat{E}}[\ell]$ as well as $\hat{D}$ are all positive.

We begin our derivation with the expression for the oscillation probability written in terms of $S(T)$, Eq. (106),

$$\mathcal{P}(\nu_a \to \nu_b) \equiv P^{ab} = |\langle M(b)|Ue^{-iH_\nu(t'-t)}U^\dagger|M(a)\rangle|^2$$
$$= \sum_{\ell\ell'} F^{ab}_{\ell\ell'} \exp^{-i(\bar{E}_\ell - \bar{E}_{\ell'})L}. \quad (71)$$

Here $F^{ab}_{\ell\ell'}$ is defined as

$$F^{ab}_{\ell\ell'} \equiv F^{ab}_\ell F^{ab*}_{\ell'} = \frac{w^{ab}_{\ell\ell'}}{\hat{\hat{D}}[\ell]\hat{\hat{D}}[\ell']} \quad (72)$$

with $\hat{\hat{D}}[\ell]$ given in Eq. (58), and

$$w^{ab}_{\ell\ell'} \equiv \langle M(b)|\hat{\hat{W}}[\ell]|M(a)\rangle\langle M(b)|\hat{\hat{W}}[\ell']|M(a)\rangle^*. \quad (73)$$

All results needed for determining exact, closed-form expressions for the partial oscillation probabilities are found in Appendix B.

As we explain in Appendix B, $w^{ab}_{\ell\ell'}$ may be expressed through four operators,

$$w^{ab}_{\ell\ell'} = w^{ab}_{0\ell\ell'} + \cos\delta_{cp} w^{ab}_{\cos\ell\ell'} + \cos^2\delta_{cp} w^{ab}_{\cos^2\ell\ell'}$$
$$+ i\sin\delta_{cp} w^{ab}_{\sin\ell\ell'}, \quad (74)$$

found from the decomposition of $\hat{\hat{W}}[\ell]$ given in Eq. (62). The quantities $w^{ab}_i[\ell]$ appearing in Eqs. (67) and (68) are the same as $w^{ab}_{i\ell\ell'}$ written in the streamlined notation,

$$w^{ab}_i[1] = w^{ab}_{i\ell\ell'} \quad \text{for } (\ell, \ell') = (3, 2)$$
$$w^{ab}_i[2] = w^{ab}_{i\ell\ell'} \quad \text{for } (\ell, \ell') = (3, 1)$$
$$w^{ab}_i[3] = w^{ab}_{i\ell\ell'} \quad \text{for } (\ell, \ell') = (2, 1), \quad (75)$$

which takes advantage of $\ell > \ell'$.

An analytic expression for $w^{ab}_{\sin}[\ell]$,

$$w^{ab}_{\sin}[\ell] = K\sin 2\theta_{23}\Delta\hat{\hat{E}}[\ell]\epsilon^{ab}_{\sin}, \quad (76)$$

follows directly from Eq. (62). Here, $\epsilon_{\sin}$ is the antisymmetric matrix

$$\epsilon_{\sin} \equiv \begin{pmatrix} 0 & 1 & -1 \\ -1 & 0 & 1 \\ 1 & -1 & 0 \end{pmatrix} \quad (77)$$

and

$$K = -\frac{\alpha(1-\alpha)}{8}$$
$$\times \cos\theta_{13}\sin 2\theta_{12}\sin 2\theta_{13}. \qquad (78)$$

Equation (76) is one of the more striking results. Analytic formulas for the other $w_i^{ab}[\ell]$ follow from Eq. (56). These are all given in Appendix B, where they are expressed in terms of the parameters specifying $\hat{\bar{H}}_{0v}$ and $\hat{H}_1 = U^{-1}\hat{V}U$. These are the same parameters defining SNM.

It follows from Eq. (76) that the coefficients of $\Delta\hat{\bar{E}}[\ell]j_0(2\hat{\Delta}[\ell])$ in Eq. (67) are all proportional, leading to a simple expression for $P_{\sin\delta}^{ab}$,

$$P_{\sin\delta}^{ab}(\Delta_L,\hat{A}) = \Delta_L^3\alpha(1-\alpha)\sin\delta_{cp}\epsilon_{\sin}^{ab}$$
$$\times \cos\theta_{13}\sin 2\theta_{12}\sin 2\theta_{13}\sin 2\theta_{23}$$
$$\times j_0(\hat{\Delta}[3])j_0(\hat{\Delta}[2])j_0(\hat{\Delta}[1]). \qquad (79)$$

Note that $P_{\sin\delta}^{ab}$ is antisymmetric under $a\leftrightarrow b$.

Analytic expressions for all other partial oscillation probabilities follow from Eq. (71) using Eq. (72), which expresses $F_{\ell\ell'}^{ab}$ in terms of $w_{\ell\ell'}^{ab}$. In this fashion, these partial oscillation probabilities are also expressed in terms of the parameters of the SNM and the neutrino eigenvalues, $\hat{\bar{E}}_\ell$.

The usefulness of the partial oscillation probabilities can be seen as follows. It is a general result that the exchange of initial and final states in the oscillation probability or neutrinos (antineutrinos) is equivalent to letting $\delta_{cp}\to -\delta_{cp}$. Thus, the result for the inverse reaction $\mathcal{P}(\nu_b\to\nu_a)$ is found by exchanging (a,b) in Eq. (66). Since $P_{\sin\delta}^{ab}$ is antisymmetric under the exchange of (a,b), and P_0^{ab}, $P_{\cos\delta}^{ab}$ and $P_{\cos^2\delta}^{ab}$ symmetric, it follows that P^{ba} is given by

$$\mathcal{P}(\nu_b\to\nu_a) = \delta(a,b) + P_0^{ab} - P_{\sin\delta}^{ab} + P_{\cos\delta}^{ab}$$
$$+ P_{\cos^2\delta}^{ab}. \qquad (80)$$

In analogy to Eq. (66), we may express the oscillation probability for antineutrinos as

$$\mathcal{P}(\bar{\nu}_a\to\bar{\nu}_b) \equiv \bar{P}^{ab} = \delta(a,b) + \bar{P}_0^{ab} + \bar{P}_{\sin\delta}^{ab} + \bar{P}_{\cos\delta}^{ab} + \bar{P}_{\cos^2\delta}^{ab}, \qquad (81)$$

where the bared probabilities for antineutrinos are obtained from the unbarred for neutrinos by replacing $\delta_{cp}\to -\delta_{cp}$ and $\hat{A}\to -\hat{A}$. Because the energies of antineutrinos are different from those of the neutrinos in matter, we can expect $P^{ab}\neq\bar{P}^{ab}$ in this situation.

Again applying the rule that exchange of initial and final states is accomplished by letting $\delta_{cp}\to -\delta_{cp}$, the

oscillation probability $\mathcal{P}(\bar{\nu}_b\to\bar{\nu}_a)$ is expressed in terms of the same four quantities,

$$\mathcal{P}(\bar{\nu}_b\to\bar{\nu}_a) = \delta(a,b) + \bar{P}_0^{ab} - \bar{P}_{\sin\delta}^{ab} + \bar{P}_{\cos\delta}^{ab} + \bar{P}_{\cos^2\delta}^{ab}. \qquad (82)$$

It is worth noting that the entire dependence of the oscillation probabilities given in Eqs. (67) and (68) on the neutrino beam energy E, the baseline L, and the medium properties occurs through the variables Δ_L and $\hat{A}$ defined in Eqs. (33) and (24), respectively. Since we will be most interested in how the neutrino oscillation probability depends on the beam energy, baseline, and medium properties, the partial oscillation probabilities have been expressed as functions of Δ_L and $\hat{A}$.

Because the vacuum result is also easily obtained by less sophisticated arguments, the vacuum limit provides an opportunity to verify our Hamiltonian formulation in a well-known special case.

D. Special cases

We next examine special cases chosen to highlight specific aspects of our formulation. Because these cases are well known in other contexts, they provide useful cross checks. We first consider two-flavor mixing and then the vacuum limit.

1. Two flavor mixing

Expressions for two-neutrino oscillations are easily obtained from the Hamiltonian,

$$\hat{\bar{H}}_\nu = \hat{\bar{H}}_{0\nu} + U^{-1}\hat{H}_{1\nu}U, \qquad (83)$$

where

$$\hat{\bar{H}}_{0\nu} \equiv \begin{pmatrix} 0 & 0 \\ 0 & 1 \end{pmatrix}, \qquad (84)$$

$$\hat{\bar{H}}_{1\nu} \equiv \begin{pmatrix} \hat{A} & 0 \\ 0 & 0 \end{pmatrix}. \qquad (85)$$

The standard mixing matrix U is

$$U \equiv \begin{pmatrix} \cos\theta & \sin\theta \\ -\sin\theta & \cos\theta \end{pmatrix}. \qquad (86)$$

The neutrino Hamiltonian is easily diagonalized to find the medium-modified two-flavor neutrino eigenvalues,

$$\hat{\bar{E}}_2 = \frac{1}{2}(1 + \hat{A} + \phi)$$

$$\hat{\bar{E}}_1 = \frac{1}{2}(1 + \hat{A} - \phi), \qquad (87)$$

where $\phi = \sqrt{1 + \hat{A}^2 - 2\hat{A}\cos 2\theta}$.

Expressed in dimensionless variables, the time-evolution operator S^{ab} for the transition $a \to b$ becomes

$$S^{ab} = \langle M(b)|U\exp^{-2i\hat{H}_\nu \Delta_L} U^{-1}|M(a)\rangle, \qquad (88)$$

with Δ_L given in Eq. (33). The two-flavor oscillation probability $P_{2f}^{12}(\Delta_L, \hat{A})$ is then

$$P_{2f}^{12}(\Delta_L, \hat{A}) = |S_{2f}^{12}|^2$$

$$= \frac{\sin^2 2\theta}{\phi^2} \sin^2 \Delta_L \phi, \qquad (89)$$

which we will next compare to our Hamiltonian formulation. To find $S_{2f}^{12} = \langle M(2)|S[L]|M(1)\rangle$, it is easy to overlook that the 2×2 matrix H_ν in Eq. (83) is not diagonal in the flavor basis.

The oscillation probability in the three neutrino mixing of our Hamiltonian formulation is matched to the two-flavor case just discussed by setting two of the mixing angles in Eq. (12) to zero, say $\theta_{13} \to 0$ and $\theta_{23} \to 0$ and identifying θ with θ_{12}. Accordingly, we find

$$U \equiv \begin{pmatrix} \cos\theta & \sin\theta & 0 \\ -\sin\theta & \cos\theta & 0 \\ 0 & 0 & 1 \end{pmatrix}. \qquad (90)$$

This is easily recognized as a two-flavor mixing matrix by noting that one of the three neutrinos does not mix with the other two. We see that it not only depends on just one mixing angle θ, but also that the dependence on the CP violating phase δ has dropped out.

Natural choices for a 3×3 two-flavor neutrino vacuum Hamiltonian and interaction are

$$\hat{H}_{0\nu} \equiv \begin{pmatrix} 0 & 0 & 0 \\ 0 & 1 & 0 \\ 0 & 0 & 0 \end{pmatrix}, \qquad (91)$$

and

$$\hat{H}_1 \equiv \begin{pmatrix} \hat{A} & 0 & 0 \\ 0 & 0 & 0 \\ 0 & 0 & 0 \end{pmatrix}. \qquad (92)$$

When the 3×3 neutrino Hamiltonian $\hat{H}_\nu = \hat{H}_{0\nu} + U^{-1}\hat{H}_{1\nu}U$ is diagonalized, two of the three medium-modified neutrino eigenvalues,

$$\hat{\bar{E}}_3 = \frac{1}{2}(1 + \hat{A} + \phi)$$

$$\hat{\bar{E}}_2 = \frac{1}{2}(1 + \hat{A} - \phi)$$

$$\hat{\bar{E}}_1 = 0, \qquad (93)$$

are identical to those found above in the two-flavor case. Note that the eigenvalues have no branch points for $\hat{A}$ on the real axis. From these eigenvalues, we find the differences,

$$\Delta\hat{\bar{E}}[3] = \hat{\bar{E}}_2 - \hat{\bar{E}}_1$$

$$= \frac{1}{2}(1 + \hat{A} - \phi)$$

$$\Delta\hat{\bar{E}}[2] = \hat{\bar{E}}_3 - \hat{\bar{E}}_1$$

$$= \frac{1}{2}(1 + \hat{A} + \phi)$$

$$\Delta\hat{\bar{E}}[1] = \hat{\bar{E}}_3 - \hat{\bar{E}}_2 = \phi. \qquad (94)$$

Finally, consider the oscillation probability in our Hamiltonian formulation. Because $P_{\sin\delta}^{ab}$, $P_{\cos\delta}^{ab}$, and $P_{\cos^2\delta}^{ab}$ are proportional to $\sin 2\theta_{23}$ (and θ_{23} has been set to 0), these terms do not contribute for two-flavor mixing. Thus,

$$P^{ab}(\Delta_L, \hat{A}) = \delta(a, b) + P_0^{ab}(\Delta_L, \hat{A}), \qquad (95)$$

with $P_0^{ab}(\Delta_L, \hat{A})$ taken from Eq. (68). We find after a straightforward calculation,

$$w_0^{11}[\ell] = -w^{12}[\ell]$$
$$w_0^{21}[\ell] = w_0^{12}[\ell]$$
$$w_0^{22}[\ell] = -w^{12}[\ell], \qquad (96)$$

where

$$w_0^{12}[\ell] = w_{02}^{(12)}(\hat{A}\cos^2\theta - (1 + \hat{A})\hat{\bar{E}}_\ell + \hat{\bar{E}}_\ell^2). \qquad (97)$$

Taking $\hat{\bar{E}}_\ell$ from Eq. (93), we evaluate

$$\hat{A}\cos^2\theta - (1 + \hat{A})\hat{\bar{E}}_\ell + \hat{\bar{E}}_\ell^2 \qquad (98)$$

to find

$$w_0^{12}[1] = w_0^{12}[2] = 0 \qquad (99)$$

and

$$w_0^{12}[3] = \hat{A}\cos^2\theta w_{0,2}^{(12)}$$

$$= \frac{\hat{A}}{4}\cos^2\theta \sin^2 2\theta. \qquad (100)$$

Thus, for all two-flavor transitions,

$$P^{ab}(\Delta_L, \hat{A}) = \delta(a,b) + \frac{4\Delta_L^2}{\hat{D}} w_0^{ab}[3]\Delta\hat{\bar{E}}[3]$$
$$\times j_0^2(\Delta\hat{\bar{E}}[3]\Delta_L), \qquad (101)$$

where $\hat{D}$ is from Eq. (102),

$$\hat{D} \equiv \Delta\hat{\bar{E}}[1]\Delta\hat{\bar{E}}[2]\Delta\hat{\bar{E}}[3]$$
$$= \frac{\Delta\hat{\bar{E}}[1]}{4}((1+\hat{A})^2 - 1 - \hat{A}^2 + 2\hat{A}\cos 2\theta)$$
$$= \hat{A}\cos^2\theta\Delta\hat{\bar{E}}[1]. \qquad (102)$$

To compare our result to the well-known two-flavor oscillation probability given in Eq. (89), we evaluate Eq. (101) for $1 \rightarrow 2$ transitions, obtaining

$$P^{12}(\Delta_L, \hat{A}) = \frac{\sin^2 2\theta}{\phi^2} \sin^2 \Delta_L \phi. \qquad (103)$$

As expected, this is in complete agreement with Eq. (89).

2. Vacuum oscillation probability

In our Hamiltonian formulation, an expression for the time-evolution operator in the vacuum limit $\hat{A} \rightarrow 0$ is found from Eqs. (52), (53), (56), and (58),

$$\langle M(b)|S^0(t',t)|M(a)\rangle \equiv S^{0ab}(t'-t)$$
$$= \sum_\ell \frac{\langle M(b)|\hat{\bar{W}}^0[\ell]|M(a)\rangle}{\hat{D}^0[\ell]} \exp^{-i\bar{E}_\ell^0\Delta_L}, \qquad (104)$$

Here, $\bar{E}_\ell^0$ and $\hat{D}^0[\ell]$ are the vacuum values of $\bar{E}_\ell$ and $\hat{D}[\ell]$, respectively. In the vacuum, of course, there is no distinction between the energy differences for neutrinos and anti-neutrinos. Evaluating Eq. (104) by inserting a complete set of states intermediate states $|n\rangle\langle n|$ inside $\hat{\bar{W}}[\ell]$, we arrive at

$$\langle M(b)|S^0(t',t)|M(a)\rangle$$
$$= \sum_\ell \sum_n U_{bn} \frac{(\hat{\bar{E}}_n^0 - \hat{\bar{E}}_a^0)(\hat{\bar{E}}_n^0 - \hat{\bar{E}}_b^0)}{\hat{D}^0[\ell]} U_{na}^* e^{-i\bar{E}_\ell^0(t'-t)}, \qquad (105)$$

The indices (a,b,n) run over all permutations of the three integers $(1,2,3)$, from which it follows that $(\hat{\bar{E}}_n^0 - \hat{\bar{E}}_{a[\ell]}^0)(\hat{\bar{E}}_n^0 - \hat{\bar{E}}_{b[\ell]}^0) \equiv \hat{D}^0[\ell]$, and, consequently,

$$\langle M(b)|S^0(t',t)|M(a)\rangle = \sum_n U_{bn} e^{-iE_n^0(t'-t)} U_{na}^*. \qquad (106)$$

This well-known vacuum limit also follows directly from more elementary considerations, using Eqs. (5) and (11),

$$\langle \nu_{fb}^0|e^{-iH_{0v}(t'-t)}|\nu_{fa}^0\rangle = \sum_n U_{bn} e^{-iE_n^0(t'-t)} U_{na}^*. \qquad (107)$$

The equality of Eqs. (106) and (110) verifies our exact Hamiltonian formulation in the vacuum limit. Finally, we find that $F_{\ell\ell'}^{ab}$ appearing Eq. (71) takes a familiar form in the vacuum. Using Eq. (106), or Eq. (110),

$$\mathcal{P}(\nu_a^0 \rightarrow \nu_b^0) = \left(\sum_\ell U_{b\ell} e^{-i\bar{E}_\ell^0(t'-t)} U_{\ell a}^*\right)$$
$$\times \left(\sum_{\ell'} U_{b\ell'} e^{-i\bar{E}_{\ell'}^0(t'-t)} U_{\ell'a}^*\right)^*. \qquad (108)$$

Expressing this in terms of Freund's $J_{\ell\ell'}^{ab}$ [4],

$$J_{\ell\ell'}^{ab} \equiv U_{b\ell}^* U_{a\ell} U_{a\ell'}^* U_{b\ell'}, \qquad (109)$$

and using Eq. (26),

$$\bar{E}_\ell^0 - \bar{E}_{\ell'}^0 = \frac{m_\ell^2 - m_{\ell'}^2}{2E}, \qquad (110)$$

we find that Eq. (108) may be written,

$$\mathcal{P}(\nu_a^0 \rightarrow \nu_b^0) = \delta_{ab} - 4\sum_{i>j} \text{Re}J_{ij}^{ab}\sin^2((\bar{E}_\ell^0 - \bar{E}_{\ell'}^0)L)$$
$$- 2\sum_{i>j} \text{Im}J_{ij}^{ab}\sin(2(\bar{E}_\ell^0 - \bar{E}_{\ell'}^0)L), \qquad (111)$$

Comparing Eqs. (111) and (71), it is clear that $F_{\ell\ell'}^{ab} \rightarrow J_{\ell\ell'}^{ab*}$ in the vacuum limit.

IV. THE STANDARD NEUTRINO MODEL

We adopt the standard neutrino model [2] as our description of neutrino physics. The parameters defining the model include a (dimensionless) interaction strength $\hat{A}$ of neutrinos and antineutrinos with matter, the three neutrino mass differences, the three mixing angles, and the *CP* violating phase. Most of the parameters of the SNM are consistent with global fits to neutrino oscillation data with relatively good precision.

The neutrino mass differences of the SNM are taken to be [7–11]

$$m_2^2 - m_1^2 \equiv \delta m_{21}^2$$
$$= 7.6 \times 10^{-5} \text{ eV}^2$$
$$m_3^2 - m_1^2 \equiv \delta m_{31}^2$$
$$= 2.4 \times 10^{-3} \text{ eV}^2, \qquad (112)$$

corresponding to

$$\alpha \equiv \frac{\delta m_{21}^2}{\delta m_{31}^2}$$
$$= 3.17 \times 10^{-2}. \qquad (113)$$

In Ref. [7–11], $\delta \equiv (m_2^2 - m_1^2)/(2E)$ and $\Delta = (m_3^2 - m_1^2)/(2E)$ whereas in Ref. [4], $\hat{\Delta} = (m_3^2 - m_1^2)L/(4E)$ and $\Delta = m_3^2 - m_1^2$.

The mixing angle θ_{23},

$$\theta_{23} = \pi/4, \tag{114}$$

is the best-fit value from Ref. [13], and θ_{12},

$$\theta_{12} = \pi/5.4, \tag{115}$$

is consistent with the recent analysis of Ref. [14]. The mixing angle θ_{13} is known to be small ($\theta_{13} < 0.18$ at the 95% confidence level) but its precise value is uncertain. A very recent result from the Daya Bay project [15] is $\sin\theta_{13} \approx 0.15$, which we adopt to determine our value for θ_{13},

$$\theta_{13} = 0.151. \tag{116}$$

The *CP* violating phase δ_{cp} is not known at all and will one of the major interests at future neutrino facilities.

Parametrizing the interaction strength $\hat{A}$, Eq. (24), we find

$$\hat{A} = \pm 6.50 \times 10^{-2} \frac{Z}{N} E[\text{GeV}]\rho[\text{gm/cm}^3], \tag{117}$$

with $E[\text{GeV}]$ being the neutrino beam energy E (in GeV) and $\rho[\text{gm/cm}^3]$, is the average total density (in gm/cm³) of matter through which the neutrino beam passes on its way to the detector (the matter having average proton-neutron ratio Z/N). For our calculations we are interested in experiments close to the Earth's surface, so we take

$$\rho[\text{gm/cm}^3] = \rho_0$$
$$= 3, \tag{118}$$

the approximate mean density of the Earth's mantle.

In the SNM, Δ_L, defined in Eq. (33), may be parametrized in the high-energy limit as

$$\Delta_L \approx 3.05 \times 10^{-3} \frac{L[\text{Km}]}{E[\text{GeV}]}. \tag{119}$$

Here $L[\text{Km}]$ is the baseline and $E[\text{GeV}]$ is the neutrino beam energy. Because $\sin^2\theta_{13}$ are small, comparable in size, and rather well determined in the SNM, it will sometimes be convenient replace $\sin^2\theta_{13} \to \alpha R_p$, where $R_p = \sin^2\theta_{13}/\alpha \approx 0.71$.

V. EIGENVALUE EXPANSIONS IN THE SNM

The fact that α and $\sin\theta_{13}$ are naturally small in the SNM commonly motivates approximation schemes [4–6,16]

based on first-order Taylor series expansions in one of these small parameters, ξ_i' (where ξ_i' stands for α or $\sin^2\theta_{13}$. For example, in Refs. [5,6] the oscillation probability is expanded in $\sin^2\theta_{13}$. Reference [4] makes use of an expansion in the small parameter α.

Although these expansions may be used effectively to simplify the theory, they come at a price [4]. This price is that neither expansion gives accurate representations for all values of the interaction strength $\hat{A}$, including values in some regions of critical importance.

In our subsequent work, we will consider simplifying the oscillation probability using the same expansions, but they will be used somewhat differently, in two stages. In the first stage, the eigenvalues are expanded, as below. In the second, the expansions will be used to simplify the oscillation probability.

In this work, the eigenvalue expansion will, of course be made before introducing R_p. For the expansion of the oscillation probabilities, R_p may be introduced before the expansion is made because of its simpler analytic structure.

A. Analytic structure of eigenvalues

The key for identifying which of the ξ_i' expansions might be appropriate over specifics ranges of $\hat{A}$ is revealed by the analytic structure of the eigenvalue $\hat{\bar{E}}_\ell(\xi)$. It is particularly important to identify the locations of its branch points when $\xi_i' = 0$. Branch points identify where a series expansion of $\hat{\bar{E}}_\ell(\xi)$, or a function of it such as $\langle F(H_\nu)\rangle$, would not converge.

We have seen that $\hat{\bar{E}}_\ell(\xi)$ depends on ξ entirely through the two functions $(U(\xi), V(\xi))$,

$$\hat{\bar{E}}_\ell(\xi) = \hat{\bar{E}}_\ell(U(\xi), V(\xi)), \tag{120}$$

where

$$U(\xi) \equiv \text{Re}[d^{1/3}]$$
$$V(\xi) \equiv \text{Im}[d^{1/3}], \tag{121}$$

with d defined in Eq. (37).

Recalling that $4\gamma^3 - \psi^2 > 0$, we conveniently write

$$U(\xi) = \frac{1}{2}(\psi + i\sqrt{4\gamma^3 - \psi^2})^{1/3} + (\psi - i\sqrt{4\gamma^3 - \psi^2})^{1/3}, \tag{122}$$

and

$$V(\xi) = \frac{1}{2i}(\psi + i\sqrt{4\gamma^3 - \psi^2})^{1/3} - (\psi - i\sqrt{4\gamma^3 - \psi^2})^{1/3}. \tag{123}$$

Branch points ξ^B clearly occur for parameter values satisfying

$$\psi^2(\xi^B) = 4\gamma^3(\xi^B). \tag{124}$$

The locations of the branch points ξ^B of $\hat{\bar{E}}_\ell(\xi)$ are found as follows for the two small-parameter choices ξ_i'.

When $\xi_i' = \alpha$, branch points as a function of the other parameters of the standard neutrino model are found from Eq. (124) with $\psi(\xi^B)$ and $\gamma(\xi^B)$ evaluated in terms of

$$a(\xi^B) = -(1 + \hat{A})$$
$$b(\xi^B) = \hat{A}\cos^2\theta_{13}$$
$$c(\xi^B) = 0, \tag{125}$$

where $\xi^B = \xi|_{\alpha=0}$. The only real solution of Eq. (124) is

$$\hat{A} = 0. \tag{126}$$

When $\xi_i' = \sin^2\theta_{13}$, branch points as a function of the other parameters of the SNM are found from Eq. (124) with $\psi(\xi^B)$ and $\gamma(\xi^B)$ evaluated in terms of

$$a(\xi^B) = -(1 + \hat{A} + \alpha)$$
$$b(\xi^B) = \alpha + \hat{A}\alpha\cos\theta_{12} + \hat{A}$$
$$c(\xi^B) = -\hat{A}\alpha\cos^2\theta_{12}, \tag{127}$$

where $\xi^B = \xi|_{\theta_{13}=0}$. The only real solution of Eq. (124) is

$$\hat{A} = \hat{A}_0 \equiv \frac{1-\alpha}{1 - \alpha\cos^2\theta_{12}}$$
$$\approx 1. \tag{128}$$

B. The first-order Taylor expansions

Defining $\hat{\bar{E}}_\ell^\xi$ to be the first two terms of the Taylor series for $\hat{\bar{E}}_\ell$ expanded about $\xi = 0$, we find

$$\hat{\bar{E}}_\ell^\xi \equiv \hat{\bar{E}}_\ell|_{\xi=0} + \xi \left.\frac{\partial\hat{\bar{E}}_\ell}{\partial\xi}\right|_{\xi=0}, \tag{129}$$

where $\hat{\bar{E}}_\ell$ and $\partial\hat{\bar{E}}_\ell/\partial\xi$ are easily obtained from Eqs. (34) and (35) and their derivatives. The results for $\xi = \sin^2\theta_{13}$ and $\xi = \alpha$ found in this way are given immediately below.

1. $\xi = \sin^2\theta_{13}$

Applying Eq. (129) we find for $\xi = \sin^2\theta_{13}$ and below the corresponding branch point,

$$\hat{E}_1^\theta = \frac{1}{2}(\hat{A} + \alpha - \hat{C}_\theta)$$
$$+ \frac{\alpha R_p \hat{A}}{2(1-y)\hat{C}_\theta}(2 - \hat{A}_0 - \alpha - \hat{C}_\theta)$$
$$+ \frac{y\alpha R_p}{2\hat{C}_\theta}(2 - 4\hat{A}_0 + \hat{A}_0^2 - 2\alpha + 2\hat{A}_0\alpha)$$

$$\hat{E}_2^\theta = \frac{1}{2}(\hat{A} + \alpha + \hat{C}_\theta)$$
$$- \frac{\alpha R_p \hat{A}}{2(1-y)\hat{C}_\theta}(2 - \hat{A}_0 - \alpha + \hat{C}_\theta)$$
$$- \frac{y\alpha R_p}{2\hat{C}_\theta}(2 - 4\hat{A}_0 + \hat{A}_0^2 - 2\alpha + 2\hat{A}_0\alpha)$$

$$\hat{E}_3^\theta = 1 + \frac{\alpha R_p \hat{A}}{1-y}, \tag{130}$$

where $y \equiv \hat{A}/\hat{A}_0$, with $\hat{A}_0 \equiv \hat{A}_0^\theta$ the location of the branch point for the $\sin^2\theta_{13}$ expansion and

$$\hat{C}_\theta = \sqrt{\hat{A}^2 + \alpha^2 - 2\hat{A}\alpha\cos 2\theta_{12}}. \tag{131}$$

Note that $\hat{E}_2^\theta = \hat{E}_1^\theta|_{\hat{C}_\theta \to -\hat{C}_\theta}$. Above the branch point, $y > 1$, $\hat{E}_3^\theta$ and $\hat{E}_2^\theta$ exchange roles.

The lack of convergence at the branch point is manifest here by inspection, i.e., by the appearance of a simple pole at $y = 1$. Although Eq. (130) would suggest a pole in all three eigenvalues, $\hat{E}_1^\theta$ is rather accurate for all values of y. The absence of a singularity in $\hat{E}_1^\theta$ can be confirmed by a simple calculation that shows the coefficient of $(1-y)^{-1}$ vanishes at $y = 1$.

2. $\xi = \alpha$

Taking $R_p = \sin^2\theta_{13}/\alpha$, we may write $\cos^2\theta_{13} = 1 - \alpha R_p$ and $\cos 2\theta_{13} = 1 - 2\alpha R_p$. Then, for $\xi = \alpha$ and $y > 0$ (above its corresponding branch point),

$$\hat{E}_1^\alpha = \alpha\cos^2\theta_{12}$$
$$\hat{E}_2^\alpha = \frac{1}{2}(1 + \hat{A} - \hat{C}_\alpha)$$
$$+ \alpha\frac{\sin\theta_{12}}{2}\left(1 + \frac{1 - \hat{A}(1 - 2\alpha R_p)}{\hat{C}_\alpha}\right)$$
$$\hat{E}_3^\alpha = \frac{1}{2}(1 + \hat{A} + \hat{C}_\alpha)$$
$$+ \alpha\frac{\sin\theta_{12}^2}{2}\left(1 - \frac{1 - \hat{A}(1 - 2\alpha R_p)}{\hat{C}_\alpha}\right), \tag{132}$$

where

$$\hat{C}_\alpha = \sqrt{(1-\hat{A})^2 + 4\alpha R_p \hat{A}}. \tag{133}$$

Note that $\hat{\bar{E}}_2^\alpha = \hat{\bar{E}}_3^\alpha|_{\hat{C}_\alpha \to -\hat{C}_\alpha}$. These expressions are identical to Eqs. (18) and (19) of Freund [4].

In contrast to $\xi = \sin^2 \theta_{13}$, the lack of convergence of the α expansion is not obvious from a casual examination of Eq. (132). Numerical comparison to the exact result confirms that $\hat{\bar{E}}_1^\alpha$ and $\hat{\bar{E}}_2^\alpha$ are poor representations of the corresponding exact results in the vicinity of the branch point at $y = 0$. However, no evidence of the branch point is apparent in $\hat{\bar{E}}_3^\alpha$, which is rather accurate for all values of y. Across the branch point at $y = 0$, $\hat{\bar{E}}_1^\alpha$ and $\hat{\bar{E}}_2^\alpha$ exchange roles.

C. Branch points and resonances

Resonances are heralded by the appearance of minima in the EV differences. Two well-known neutrino resonances occur in the SNM. One of these, the *solar* resonance, is found for relatively weak interaction strengths $\hat{A} \approx \alpha$. The other, the *atmospheric* resonance, occurs for stronger interactions, $\hat{A} \approx \cos 2\theta_{13}$. The solar resonance occurs very close to the branch point identified with the α expansion, and the atmospheric resonance very close to the branch point identified with the $\sin^2 \theta_{13}$ expansion.

Using Eq. (117), the solar resonance appears for neutrinos of energy,

$$E = E^{\mathrm{sol}}[\mathrm{GeV}] \approx 0.325, \qquad (134)$$

for underground experiments in the Earth's mantle ($\rho[\mathrm{gm/cm^3}] = \rho_0 \approx 3$). We find, similarly, that for neutrinos of energy E, the solar resonance occurs in matter of density,

$$\rho^{\mathrm{sol}}[\mathrm{gm/cm^3}] \approx E[\mathrm{GeV}]^{-1}, \qquad (135)$$

taking $\alpha = 0.0317$ from the SNM.

Likewise, the atmospheric resonance is found for neutrinos of energy,

$$E = E^{\mathrm{atm}}[\mathrm{GeV}] \approx 9.79, \qquad (136)$$

also for underground experiments in the Earth's mantle. At energy E, it occurs at a density of

$$\rho^{\mathrm{atm}}[\mathrm{gm/cm^3}] \approx 29.4/E[\mathrm{GeV}], \qquad (137)$$

taking $\cos 2\theta_{13} = 0.955$ from the SNM.

Because of the close correlation between the branch points and the resonances, there is also a close correlation between resonances and viable approximation schemes. Note, however, that the branch point in the α expansion near the solar resonance affects both neutrino and antineutrino scattering since its actual location is $\alpha = 0$.

D. Discussion

We have seen in this section that expansions of the eigenvalues in a small parameter ξ_i' of the SNM (where ξ_i' stands for α or $\sin^2 \theta_{13}$) must be made carefully, since the EV are not analytic everywhere.

Nevertheless, as noted, first-order Taylor series representations of the EV are commonly used to simplify the theory. Because these expansions do not give an accurate representation the EV for all values of the interaction strength $\hat{A}$, it is important to identify the regions where the theoretical errors of the expanded EV might be acceptable and lead to accurate representations. We address this in the next section.

VI. APPROXIMATING $\mathcal{P}(\nu_i \to \nu_f)$ WITH EXPANDED EV

In this section, we begin our assessment of common procedures used to simplify calculation of the oscillation probability by expanding it in one of the small parameters of the SNM. Freund observed [4] that the α-expansion, although useful, could not be used near the solar resonance where $\hat{A} = \alpha$. However, no understanding of the limitations of the $\sin^2 \theta_{13}$-expansion appears in the literature.

We have shown above that the applicability of both expansions is limited by the presence of branch points in the analytical structure of the eigenvalues. The branch point responsible for the failure of the α expansion is located at $\hat{A} = 0$ when $\alpha = 0$, and the branch point responsible for the failure of the $\sin^2 \theta_{13}$ expansion is located at $\hat{A} = \hat{A}_0$ when $\sin^2 \theta_{13} = 0$, where $\hat{A}_0$ is defined in Eq. (128).

We make our assessment numerically, comparing the oscillation probability calculated from Eqs. (68) and (79) using the exact eigenvalues to that calculated from Eqs. (68) and (79) using eigenvalues expanded in one of the small parameters of the SNM.

A. Assessing oscillation probabilities expressed in terms of ξ-expanded eigenvalues

Theoretical errors characterizing an approximation scheme may emerge numerically only from an examination of the dependence of $P^{e\mu}(\Delta_L, \hat{A})$ on Δ_L and $\hat{A}$. In this section we discuss how we will do this.

It is convenient to discuss the oscillation pattern in terms of the location of the first maxima of the functions $\Delta_L j_0(\hat{\Delta}_\ell)$ appearing in the expressions for the partial oscillation probabilities. These peaks occur at $\Delta_L = \Delta_L^{(\ell)}$, with

$$\Delta_L^{(\ell)} = \frac{\pi}{2\Delta\hat{\bar{E}}[\ell]} \qquad (138)$$

closely related to the period P_ℓ of $j_0(\hat{\Delta}_\ell)$,

$$P_\ell \equiv 4\Delta_L^{(\ell)} = \frac{2\pi}{\Delta\hat{\hat{E}}[\ell]}. \qquad (139)$$

Because the exact eigenvalues never cross, the ordering of $\hat{\hat{E}}_\ell$ is the same as it is in the vacuum, namely $\hat{\hat{E}}_3 > \hat{\hat{E}}_2 > \hat{\hat{E}}_1$. It can inferred from this that all $\Delta\hat{\hat{E}}[\ell]$ remain positive, and, in addition, that

$$\Delta\hat{\hat{E}}[2] > \Delta\hat{\hat{E}}[3] > 0$$
$$\Delta\hat{\hat{E}}[2] > \Delta\hat{\hat{E}}[1] > 0. \qquad (140)$$

We see, in general, that for small $\hat{A}$, $\Delta\hat{\hat{E}}[1] > \Delta\hat{\hat{E}}[3]$, and, for large $\hat{A}$, $\Delta\hat{\hat{E}}[2] > \Delta\hat{\hat{E}}[3]$.

It is also clear that $\Delta\hat{\hat{E}}[2]$ is always the largest eigenvalue difference. Consequently, P_2 is always the smallest of the three periods, thus, characterizing the most rapidly varying Bessel function. The relative sizes of P_ℓ are easily worked out in specific cases. In the vacuum,

$$P_1 = 2\pi/(1-\alpha)$$
$$P_2 = 2\pi$$
$$P_3 = 2\pi/\alpha, \qquad (141)$$

evaluated from differences of the vacuum eigenvalues appearing in Eq. (29).

In the SNM, we find that

$$P_3 > P_1 \quad \text{for } \hat{A} < \hat{A}_2$$
$$P_1 > P_3 \quad \text{for } \hat{A} > \hat{A}_2, \qquad (142)$$

where

$$\hat{A}_2 = 0.538 \qquad (143)$$

is the value of $\hat{A}$ at which $P_3 = P_1$ ($\Delta\hat{\hat{E}}[1] = \Delta\hat{\hat{E}}[3]$).

With $\Delta\hat{\hat{E}}[2]$ the largest eigenvalue difference, P_2 is always the smallest of the three periods. Thus, the value of Δ_L at the first peak of $\Delta_L j_0(\hat{\Delta}_2)$ is a natural scale.

B. Regions of maximum sensitivity

Sensitivity to the approximation scheme should be most manifest within regions where all three Bessel functions of $P^{ab}(\Delta_L, \hat{A})$ are of similar size and interfere. This will happen once Δ_L becomes comparable to the first peak of its most slowly varying $\Delta_L j_0(\hat{\Delta}_\ell)$, which occurs at either $\Delta_L = \Delta_L^{(3)}$ or $\Delta_L = \Delta_L^{(1)}$. In general, the sensitivity to approximations increases as the distance Δ_L to the most distant peak increases.

In the vacuum, the first peak of the most slowly varying $\Delta_L j_0(\hat{\Delta}_\ell)$ is always at $\Delta_L = \Delta_L^{(3)}$, readily established by the vacuum eigenvalue differences given in Eq. (29). The

corresponding baseline is obtained from Eqs. (33) and (138), $L^{(3)}[\text{Km}] \approx 5170\pi E[\text{GeV}]$.

In the SNM, the most slowly varying Bessel function, established from Eqs. (142) and (143), is $\Delta_L j_0(\hat{\Delta}_3)$ when $\hat{A} < \hat{A}_2$ and $\Delta_L j_0(\hat{\Delta}_1)$ for $\hat{A} > \hat{A}_2$.

1. Regions of maximum sensitivity for fixed $\hat{A}$

Consider first the variation of $P^{(ab)}(\Delta_L, \hat{A})$ with Δ_L for a given value of $\hat{A}$ in the SNM.

According to Eq. (142), for $\hat{A} > \hat{A}_2$, $\Delta_L j_0(\hat{\Delta}_1)$ is the most slowly varying (having the larger period), and the region of maximum sensitivity is

$$\Delta_L > \Delta_L^{(1)} \equiv \frac{\pi}{2\Delta\hat{\hat{E}}[1]} \qquad (144)$$

with $\Delta\hat{\hat{E}}[1]$ evaluated at $\hat{A}$.

Similarly, for $\hat{A} < \hat{A}_2$, $\Delta_L j_0(\hat{\Delta}_3)$ is the most slowly varying. According to Eq. (138), its peak occurs where $\Delta_L = \pi/(2\Delta\hat{\hat{E}}[3])$. Thus, the region of maximum sensitivity is

$$\Delta_L > \Delta_L^{(3)} \equiv \frac{\pi}{2\Delta\hat{\hat{E}}[3]} \qquad (145)$$

with $\Delta\hat{\hat{E}}[3]$ again evaluated at $\hat{A}$.

2. Regions of maximum sensitivity for fixed Δ_L

Consider next the variation of $P^{(ab)}(\Delta_L^0, \hat{A})$ with $\hat{A}$ for given Δ_L^0 in the SNM.

According to Eq. (142), for $\hat{A} > \hat{A}_2$, $\Delta_L j_0(\hat{\Delta}_1)$ is the most slowly varying. According to Eq. (138), its peak occurs where $\Delta_L^0 = \pi/(2\Delta\hat{\hat{E}}[1])$. Thus, the region of maximum sensitivity is

$$\Delta\hat{\hat{E}}[1] > \frac{\pi}{2\Delta_L^0} \qquad (146)$$

with $\Delta\hat{\hat{E}}[1]$ evaluated at $\hat{A}$.

Similarly, for $\hat{A} < \hat{A}_2$, we find from Eq. (144) that $\Delta_L j_0(\hat{\Delta}_3)$ is the most slowly varying, and the region of maximum sensitivity is

$$\Delta\hat{\hat{E}}[3] > \frac{\pi}{2\Delta_L^0}. \qquad (147)$$

VII. NUMERICAL STUDY OF $\mathcal{P}(\nu_e \to \nu_\mu)$ WITH EXPANDED EV

Our main interest in the present section is to map out the regions where each of the small-parameter expansions is capable of simplifying $P^{ab}(\Delta_L, \hat{A})$. We do this by

comparing three calculations using $\mathcal{P}(\nu_e \to \nu_\mu)$ taken from our exact Hamiltonian formulation.

One of these is a calculation of the exact oscillation probability obtained in our Hamiltonian formulation. For this we use the expressions in Eqs. (67) and (68) evaluated with the exact EV. The other two are calculations of our ξ-expanded oscillation probability for each of the small parameters of the SNM. For these we evaluate Eqs. (67) and (68) using the ξ-expanded EV. For $\xi = \alpha$, we use the α-expanded EV given in Eq. (132), and for $\xi = \sin^2 \theta_{13}$ we use the $\sin^2 \theta_{13}$-expanded EV given in Eq. (130). The calculation with the ξ-expanded EV would, of course, coincide with the exact calculation in the vacuum. Differences, therefore, reflect medium effects.

The extent to which our oscillation probability evaluated with one of the ξ-expanded EV agrees with the exact result indicates regions in which it may be possible to obtain, at least in principle, a simple ξ-expanded expression for the oscillation probability in good agreement with the exact result. In a subsequent paper [17], we make a similar comparison between the exact oscillation probability and the approximate ones given in Refs. [4,5].

From the numerical results we obtain in Ref. [17] and the present paper, we will be able to identify regions in which both (1) the exact oscillation probability and the results of Refs. [4,5] are in poor agreement; and, (2) the exact oscillation probability and the ξ-expanded result are in excellent agreement. The regions where both of these conditions are satisfied indicate where it might be possible to improve the results found in Refs. [4,5] using our Hamiltonian formulation. We explore this possibility in yet another paper [18].

Equations (33), (117) provide a means to extrapolate the results in any figure to a variety of baseline values, medium properties, and neutrino energies within the particular regions shown in that figure. In the Earth's mantle, where the average $Z/N = 1/2$, Eqs. (117) and (33) become

$$L[\text{Km}] = 1.08 \times 10^4 \frac{\hat{A}\Delta_L}{\rho[\text{gm/cm}^3]}$$

$$E[\text{GeV}] = 30.8 \frac{\hat{A}}{\rho[\text{gm/cm}^3]}. \tag{148}$$

A. Δ_L dependence of $\mathcal{P}(\nu_e \to \nu_\mu)$

We begin our exploration of the extent to which a particular ξ expansion is capable of simplifying the oscillation probability by examining $P^{(e\mu)}(\Delta_L, \hat{A})$ vs Δ_L for particular values of $\hat{A}$. One value of $\hat{A}$ is chosen near the solar resonance and another near the atmospheric resonance. For each choice of ξ and $\hat{A}$, we compare the exact result to Eq. (129).

We first examine $\mathcal{P}(\nu_e \to \nu_\mu)$ below the solar resonance, at $\hat{A} = 0.0102$. For this value of $\hat{A}$, $\Delta\hat{\bar{E}}[3] \approx 0.0294$,
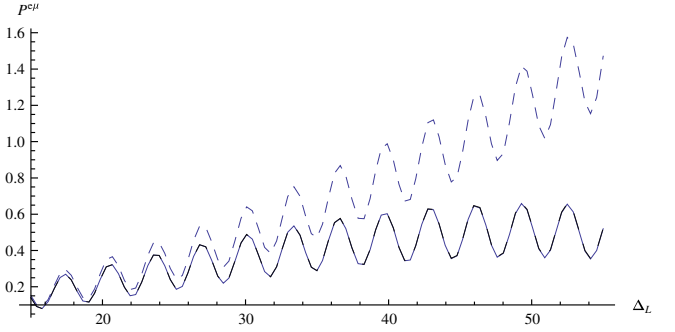

FIG. 1 (color online). $P^{e\mu}(\Delta_L, \hat{A})$ in the solar-resonance region ($\hat{A} = 0.0102$) over the interval $15 < \Delta_L < 55$ for neutrinos in matter. Parameters are taken from the SNM. Exact result (solid curve). Our expression for the oscillation probability evaluated with the α-expanded EV (medium-dashed curve). Our expression for the oscillation probability evaluated with the $\sin^2 \theta_{13}$-expanded EV (long-dashed curve).

Eq. (145) specifies that the approximate oscillation probability becomes sensitive to approximations for $\Delta_L > \Delta_L^{(3)} \approx 53$.

Our calculations for $\hat{A} = 0.0102$ are shown in Fig. 1. We see from this figure that the α-expanded oscillation probability begins to departs from the exact result at large Δ_L meaning, as expected, that the α expansion breaks down in the vicinity of the solar resonance. The sensitivity to medium effects shows up already for $\Delta_L \approx 20$, which is smaller than $\Delta_L^{(3)} \approx 53$ estimated using Eq. (145). On the other hand, Eq. (129) evaluated with eigenvalues expanded to first order in $\sin^2 \theta_{13}$ agree well with the exact result at large Δ_L showing that the $\sin^2 \theta_{13}$-expanded oscillation probability is capable of providing an excellent approximation in the vicinity of the solar resonance.

For this small value of $\hat{A}$, we find that position of the first peak of the exact oscillation probability, $\Delta_L \approx 1.58$, coincides almost exactly with the location of the peak of the most rapidly varying Bessel function, $j_0(\hat{\Delta}_2)$. From Eq. (148), we note that the oscillation probability at $\Delta_L = 20$ in Fig. 1, where the approximate calculation begins to break down in the solar resonance region with the α-expanded EV, would correspond to a measurement of 105 MeV neutrinos propagating in the Earth's mantle at a baseline 734 Km.

We next examine $\mathcal{P}(\nu_e \to \nu_\mu)$ for $\hat{A} = 0.8$, a value of $\hat{A}$ near the atmospheric resonance. Taking the exact eigenvalue difference $\Delta\hat{\bar{E}}[1] \approx 0.328$ at $\hat{A} = 0.8$, Eq. (144) specifies that the desired sensitivity of the oscillation probability to approximations should become apparent at $\Delta_L \approx 4.8$. Our calculations for $\hat{A} = 0.8$ are shown in Fig. 2.

The exact result shown in Fig. 2 (solid curve) begins to differ from the $\sin \theta_{13}$-expanded result (long-dashed curve) at $\Delta_L \approx 2$, which occurs a bit before $\Delta_L \approx 4.8$, where all three Bessel functions fully contribute. Because the long-dashed curve begins to depart from the solid curve at large
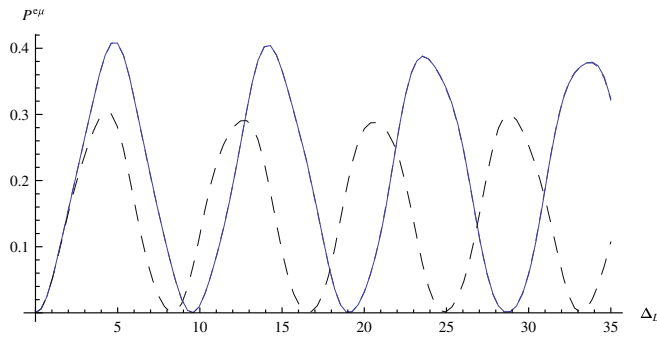
FIG. 2 (color online). $P^{e\mu}(\Delta_L, \hat{A})$ in the atmospheric resonance region ($\hat{A} = 0.8$) over the interval $0 < \Delta_L < 35$ for neutrinos in matter. Parameters are taken from the SNM. Exact result (solid curve). Our expression for the oscillation probability evaluated with the α-expanded EV (medium-dashed curve).

Δ_L, these results confirm that $P^{e\mu}(\Delta_L, \hat{A})$ evaluated with $\sin^2 \theta_{13}$-expanded EV breaks down near the atmospheric resonance with medium effects included. The failure of the $\sin \theta_{13}$ expansion becomes increasingly apparent as Δ_L increases to larger Δ_L.

The fact that the exact result (solid curve) and α-expanded result (medium-dashed curve) seem to completely overlap demonstrates that $P^{e\mu}(\Delta_L, \hat{A})$ evaluated with the α-expanded EV is capable of becoming a completely acceptable approximation near the atmospheric resonance.

For this larger value of $\hat{A}$, the first peak of the oscillation probability, at $\Delta_L \approx 1.58$, nearly coincides with the peak of the most rapidly varying Bessel function, $j_0(\hat{\Delta}_2)$, at $\Delta_L \approx 1.5$. Applying Eq. (148), we see that the oscillation probability at the value of Δ_L where medium effects begin to become apparent in Fig. 2 would correspond to neutrinos of energy $E[\text{GeV}] \approx 4.5$ propagating in matter of density similar to the average density of the entire earth, $\rho[\text{gm/cm}^3] = 5.52$ at a baseline of 7830 Km (for comparison, the average earth radius is 6370 Km).

B. $\hat{A}$ dependence of $\mathcal{P}(\nu_e \rightarrow \nu_\mu)$

We next compare oscillation probabilities over various ranges of $\hat{A}$. For a given range of $\hat{A}$, whether or not the three Bessel functions maximally interfere depends on the choice of Δ_L, which is determined by Eqs. (146) and (147) depending on whether $\hat{A} > \hat{A}_2$ or $\hat{A} < \hat{A}_2$, respectively.

1. $0 < \hat{A} < 0.2$

Numerical studies using Eqs. (146) and (147) show that for $0 < \hat{A} < 0.2$ taking $\Delta_L = 60$ is sufficient to ensure that the three Bessel functions maximally interfere. In Fig. 3, we compare the oscillation probabilities in this region. These results confirm that the expansion in $\sin^2 \theta_{13}$ is a reasonably good approximation within the solar resonance region, whereas the expansion in α is evidently not.
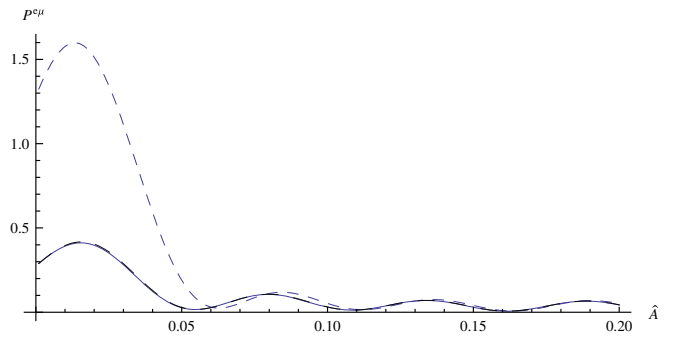

FIG. 3 (color online). $P^{e\mu}(\Delta_L, \hat{A})$ for $\Delta_L = 60$ over the interval $0 < \hat{A} < 0.2$, for neutrinos in matter. Parameters are taken from the SNM. Exact result (solid curve). Our expression for the oscillation probability evaluated with the α-expanded EV (medium-dashed curve). Our expression for the oscillation probability evaluated with the $\sin^2 \theta_{13}$-expanded EV (long-dashed curve).

2. $0.2 < \hat{A} < \hat{A}_2$

Numerical studies using Eqs. (146) and (147) show that for $0 < \hat{A} < \hat{A}_2$ taking $\Delta_L = 10$ is sufficient to ensure that the three Bessel functions maximally interfere. In Fig. 4, we compare the oscillation probabilities in this region. These results confirm that both the expansion in $\sin^2 \theta_{13}$ and the expansion in α are reasonably good approximations here.

Results shown here apply over the same range of neutrino energy, baselines, and medium properties as those given in Eqs. (148). The extrapolation applies, of course, only within the region $0.2 < \hat{A} < \hat{A}_2$.

3. $\hat{A}_2 < \hat{A} < 0.8$

Numerical studies using Eqs. (146) and (147) show that for $\hat{A}_2 < \hat{A} < 0.8$ taking $\Delta_L = 4$ is sufficient to ensure that the three Bessel functions maximally interfere. In Fig. 5, we compare the oscillation probabilities over this region.
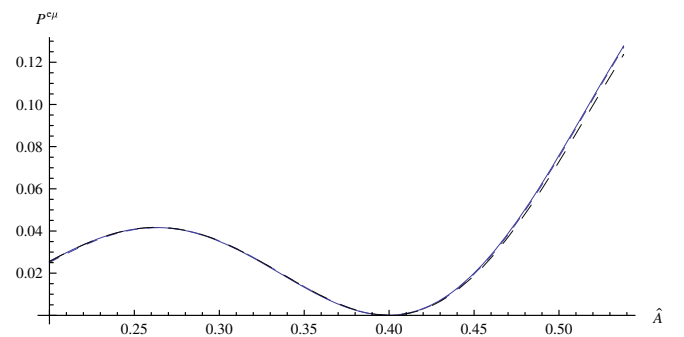

FIG. 4 (color online). $P^{e\mu}(\Delta_L, \hat{A})$ for $\Delta_L = 10$ over the interval $0.2 < \hat{A} < \hat{A}_2$, for neutrinos in matter. Parameters are taken from the SNM. Exact result (solid curve). Our expression for the oscillation probability evaluated with the α-expanded EV (medium-dashed curve). Our expression for the oscillation probability evaluated with the $\sin^2 \theta_{13}$-expanded EV (long-dashed curve).
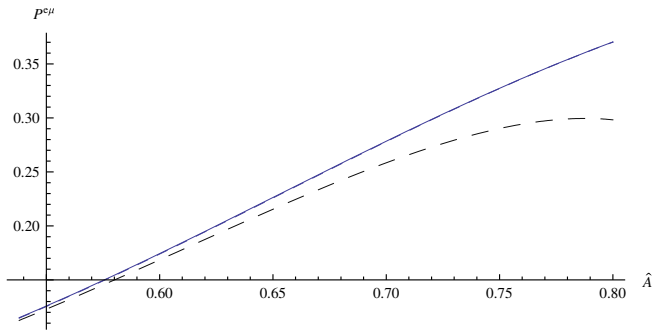
FIG. 5 (color online). $P^{e\mu}(\Delta_L, \hat{A})$ for $\Delta_L = 4$ over the interval $\hat{A}_2 < \hat{A} < 0.8$, for neutrinos in matter. Parameters are taken from the SNM. Exact result (solid curve). Our expression for the oscillation probability evaluated with the α-expanded EV (medium-dashed curve). Our expression for the oscillation probability evaluated with the $\sin^2\theta_{13}$-expanded EV (long-dashed curve).

These results confirm that the expansion in α is a reasonably good approximation below the atmospheric resonance. The onset of the failure of the $\sin^2\theta_{13}$-expanded EV near the atmospheric resonance begins to become visible for $\hat{A} > \hat{A}_2$. Results shown here apply over the same range of neutrino energy, baselines, and medium properties as those given in Eqs. (148). The extrapolation applies, of course, only for $\hat{A}_2 < \hat{A} < 0.8$.

4. $\hat{0}.8 < \hat{A} < 1.2$

Numerical studies using Eqs. (146) and (147) show that for $\hat{0}.8 < \hat{A} < 1.2$ taking $\Delta_L = 4$ is sufficient to ensure that the three Bessel functions maximally interfere. In Fig. 6, we compare the oscillation probabilities over this region. These results confirm that the expansion in α is a reasonably good approximation across the atmospheric resonance. The $\sin^2\theta_{13}$-expanded oscillation probability is
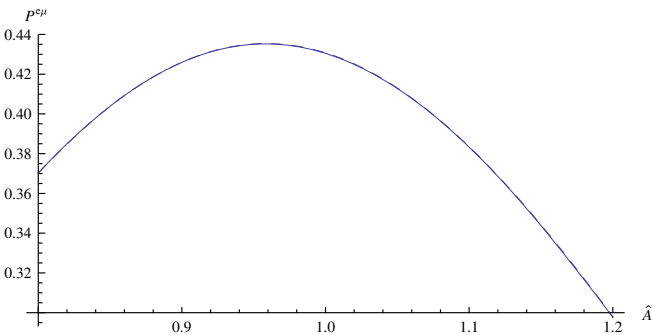

FIG. 6 (color online). $P^{e\mu}(\Delta_L, \hat{A})$ for $\Delta_L = 4$ over the interval $0.8 < \hat{A} < 1.2$, for neutrinos in matter. Parameters are taken from the SNM. Exact result (solid curve). Our expression for the oscillation probability evaluated with the α-expanded EV (medium-dashed curve). Our expression for the oscillation probability evaluated with the $\sin^2\theta_{13}$-expanded EV (long-dashed curve).
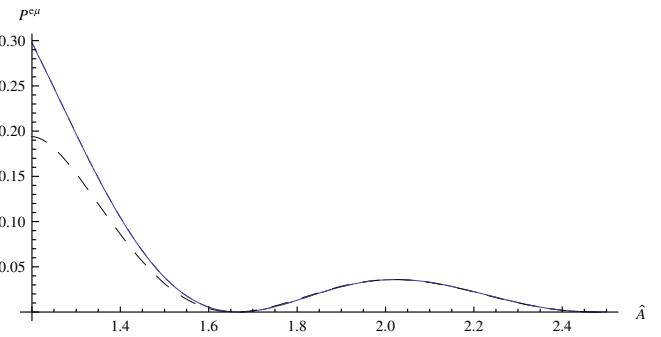

FIG. 7 (color online). $P^{e\mu}(\Delta_L, \hat{A})$ *vs* $\hat{A}$ for neutrinos in matter over the interval $1.2 < \hat{A} < 2.5$ taking $\Delta_L = 4$. Parameters are taken from the SNM. Exact result (solid curve). Our expression for the oscillation probability evaluated with the α-expanded EV (medium-dashed curve). Our expression for the oscillation probability evaluated with the $\sin^2\theta_{13}$-expanded EV (long-dashed curve).

not shown because it fails here. Results shown here apply over the same range of neutrino energy, baselines, and medium properties as those given in Eqs. (148). The extrapolation applies, of course, only for $0.8 < \hat{A} < 1.2$.

5. $1.2 < \hat{A} < 2.5$

Numerical studies using Eqs. (146) show that for $1.2 < \hat{A} < 2.5$ taking $\Delta_L = 4$ is sufficient to ensure that the three Bessel functions maximally interfere. In Fig. 7, we compare the oscillation probabilities over this region. These results show that $P^{e\mu}(\Delta_L, \hat{A})$ evaluated with the α-expanded EV is relatively accurate here. The $\sin^2\theta_{13}$-expanded oscillation probability agrees with the exact result reasonably well for $\hat{A} > 1.6$.

From Eq. (148), we see that with the value $\Delta_L = 4$, and in matter of mean density similar to that of the average density of the entire earth, $\rho[\text{gm}/\text{cm}^3] = 5.52$, the
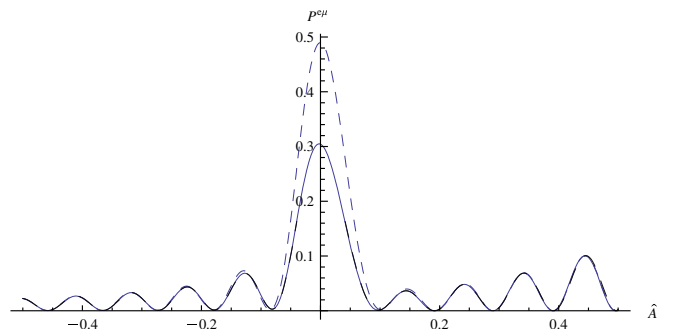

FIG. 8 (color online). $P^{e\mu}(\Delta_L, \hat{A})$ for $\Delta_L = 35$ over the interval $-0.5 < \hat{A} < 0.5$, for neutrinos and antineutrinos in matter. Parameters are taken from the SNM. Exact result (solid curve). Our expression for the oscillation probability evaluated with the α-expanded EV (medium-dashed curve). Our expression for the oscillation probability evaluated with the $\sin^2\theta_{13}$-expanded EV (long-dashed curve).

breakdown of the $\sin^2 \theta_{13}$-expanded EV starts to becomes less visible for $\hat{A} > 1.2$, corresponding to neutrinos of energy $E[\text{GeV}] \approx 6.2$ and baselines greater than $L[\text{Km}] = 23,500$ (considerably larger than the diameter of the Earth).

6. $-0.5 < \hat{A} < 0.5$

In Fig. 8, we compare the oscillation probability calculated with the exact eigenvalues to the oscillation probability calculated with the expanded eigenvalues for $-0.5 < \hat{A} < 0.5$, taking $\Delta_L = 35$. Figure 8 confirms the earlier observations that the expansion in $\sin^2 \theta_{13}$ is a valid approximation within the solar resonance region, whereas the expansion in α is not for both neutrinos and antineutrinos.

C. Intrinsic limitations

It is important to note that when using expanded EV, the range of validity of the oscillation probability $P^{ab}(\Delta_L, \hat{A})$ is limited even when it is evaluated using the convergent eigenvalue expansion. This arises because the error in the phase of the trigonometric functions $\sin(\Delta_L \Delta \hat{\bar{E}}^\xi[\ell])$ grows with Δ_L. Eventually, with increasing Δ_L, the error in the phase will lead to an unacceptable error in $P^{ab}(\Delta_L, \hat{A})$.

When spurious effects of this type would show up from a comparison of the exact partial oscillation probability evaluated with the exact $\hat{\bar{E}}_\ell$ to the exact partial oscillation probability evaluated with the convergent expansion of $\hat{\bar{E}}_\ell$. A divergence between the calculated results of these two calculations herald the limit of Δ_L beyond which the use of expanded eigenvalues breaks down for $P^{ab}(\Delta_L, \hat{A})$.

It is clear from Fig. 1 that the region of validity for both the $\sin^2 \theta_{13}$ expansion and the α expansion extend out as far as $\Delta_L = 35$.

D. Discussion

The results of this section suggest a natural division of the full range of $\hat{A}$ into regions. One significant region, which we call the *solar* resonance region, covers the range $0 < \hat{A} < 0.2$. The solar-resonance region contains, of course, the solar resonance at $\hat{A} = \alpha$. Another is the atmospheric resonance region containing the atmospheric resonance at $\hat{A} \approx \cos 2\theta_{13}$. This region covers the interval $\hat{A}_2 < \hat{A} < 2.0$.

The region between the solar and atmospheric regions, $0.2 < \hat{A} < \hat{A}_2$, is a *transition* region in the sense that within it the expansion in α is improving rapidly and the expansion in $\sin^2 \theta_{13}$ rapidly deteriorating. Within this region, the EV expansions in $\sin^2 \theta_{13}$ and α are of comparable accuracy. The *asymptotic* region covers the interval $\hat{A} > 2.0$, where the EVs are approaching their asymptotic behavior.

In future work, we will make a comparison of the our oscillation probability evaluated with the exact eigenvalues to the approximate oscillation probability given in Refs. [4,5]. By comparing those results to our oscillation probability evaluated with ξ-expanded EV found in the present paper, we will be able to identify regions where our Hamiltonian formulation might lead to more effective approximations. Based on this information, we will subsequently present any new approximate results we believe be helpful.

VIII. SUMMARY AND CONCLUSIONS

We have presented exact, closed-form expressions for the neutrino oscillation probabilities in matter using our Hamiltonian formulation within the framework of the standard neutrino model assuming three Dirac neutrinos. Our goal is to benchmark approximate formulations having known difficulties arising from expansions commonly used to model neutrino and antineutrino experiments envisioned for future neutrino facilities.

We have shown explicitly that for small α and $\sin \theta_{13}$ there are branch points in the analytic structure of the eigenvalues that lead to singular behavior of expansions near the solar and atmospheric resonance. The numerical calculations presented indicate regions in which the small-parameter expansions are guaranteed to fail and should be avoided in practice.

APPENDIX A: TIME EVOLUTION OPERATOR $S(T)$ IN OUR HAMILTONIAN FORMULATION

Our Hamiltonian formulation was presented in Sec. III A. In this appendix, and in accord with the discussion in Sec. III A, we give explicit analytic formulas for the time-evolution operator $S(L) = e^{-i\hat{H}_\nu \Delta_L}$ in terms of $\hat{\bar{E}}_\ell$ and the parameters defining $\hat{H}_\nu$.

1. Expression for $S(T)$ in terms of F_ℓ^{ab}

Introducing dimensionless variables, the time-evolution operator $S(T)$ in Eq. (106) may be written,

$$S^{ab}(L) = \sum_\ell F_\ell^{ab} \cos 2\hat{\bar{E}}_\ell \Delta_L$$
$$- i \sum_\ell F_\ell^{ab} \sin 2\hat{\bar{E}}_\ell \Delta_L. \qquad (A1)$$

Here F_ℓ^{ab}, defined in Eq. (54), may be found by evaluating Eq. (A1) at $L = 0$ and obeys the normalization condition

$$\delta_{ab} = \sum_\ell F_\ell^{ab}. \qquad (A2)$$

Using the identity $\cos 2\beta \equiv 1 - 2\sin^2 \beta$, we write

$$
\begin{aligned}
S^{ab}(L) &= \sum_\ell F_\ell^{ab}(1 - 2\sin^2 \hat{\bar{E}}_\ell \Delta_L) \\
&\quad - i\sum_\ell F_\ell^{ab} \sin 2\hat{\bar{E}}_\ell \Delta_L \\
&= \sum_\ell F_\ell^{ab} - 2\sum_\ell F_\ell^{ab} \sin^2 \hat{\bar{E}}_\ell \Delta_L \\
&\quad - i\sum_\ell F_\ell^{ab} \sin 2\hat{\bar{E}}_\ell \Delta_L.
\end{aligned} \tag{A3}
$$

Now, using the normalization, Eq. (A2),

$$
\begin{aligned}
S^{ab}(L) &= \delta_{ab} - 2\sum_\ell F_\ell^{ab} \sin^2 \hat{\bar{E}}_\ell \Delta_L \\
&\quad - i\sum_\ell F_\ell^{ab} \sin 2\hat{\bar{E}}_\ell \Delta_L.
\end{aligned} \tag{A4}
$$

Thus, for calculating $P^{ab}(L)$ in Eq. (63),

$$
\begin{aligned}
\mathrm{Re}[S^{ab}(t',t)] &= \delta_{ab} - 2\sum_\ell \mathrm{Re}[F_\ell^{ab}] \sin^2 \hat{\bar{E}}_\ell \Delta_L \\
&\quad + \sum_\ell \mathrm{Im}[F_\ell^{ab}] \sin 2\hat{\bar{E}}_\ell \Delta_L \\
\mathrm{Im}[S^{ab}(t',t)] &= -2\sum_\ell \mathrm{Im}[F_\ell^{ab}] \sin^2 \hat{\bar{E}}_\ell \Delta_L \\
&\quad - \sum_\ell \mathrm{Re}[F_\ell^{ab}] \sin 2\hat{\bar{E}}_\ell \Delta_L.
\end{aligned} \tag{A5}
$$

2. Analytic expressions for $\hat{\bar{W}}_0[\ell]$, $\hat{\bar{W}}_{\sin}[\ell]$, and $\hat{\bar{W}}_{\cos}[\ell]$ in terms of H_ν

In this appendix we give exact, analytic expressions the $S(T)$ in terms of $\hat{\bar{E}}_\ell$ and the parameters defining $\hat{\bar{H}}_\nu$. We begin with Eq. (57), which expresses F_ℓ^{ab} in terms of an operator $\hat{\bar{W}}[\ell]$ and most easily accomplish our goal by making the following rearrangement of terms in $\hat{\bar{W}}[\ell]$,

$$
\begin{aligned}
\hat{\bar{W}}[\ell] &= U\hat{\bar{H}}_{0v}^2 U^\dagger - U\hat{\bar{H}}_{0v} U^\dagger \Sigma[\ell] \\
&\quad + U\hat{\bar{H}}_{0v} U^\dagger \hat{V} + \hat{V} U\hat{\bar{H}}_{0v} U^\dagger \\
&\quad + \hat{V}^2 - \hat{V}\Sigma[\ell] + \mathbf{1}\Pi[\ell].
\end{aligned} \tag{A6}
$$

Here, $\Sigma[\ell]$ is the sum, and $\Pi[\ell]$ the product, of two EV as defined in Eqs. (42) and (43).

It is useful to recall that $\Sigma[\ell]$ and $\Pi[\ell]$, defined in this fashion, depend on ℓ entirely through $\hat{\bar{E}}_\ell$. In particular [19], from Eq. (44),

$$
\Sigma[\ell] = -a - \hat{\bar{E}}_\ell, \tag{A7}
$$

and, from Eq. (47),

$$
\Pi[\ell] = b + a\hat{\bar{E}}_\ell + \hat{\bar{E}}_\ell^2, \tag{A8}
$$

with a, b given in Eq. (35).

Explicit expressions for $\hat{\bar{W}}[\ell]$ are easily found in terms of H_ν using Eq. (A6), from which it follows that its entire dependence on δ_{cp} occurs through three operators, $W_0[\ell]$, $W_{\cos}[\ell]$ and $W_{\sin}[\ell]$,

$$
\begin{aligned}
\hat{\bar{W}}[\ell] &= \hat{\bar{W}}_0[\ell] + \cos \delta_{cp} \hat{\bar{W}}_{\cos}[\ell] \\
&\quad + i\sin \delta_{cp} \hat{\bar{W}}_{\sin}[\ell],
\end{aligned} \tag{A9}
$$

with $\hat{\bar{W}}_0[\ell]$, $\hat{\bar{W}}_{\cos}[\ell]$ and $\hat{\bar{W}}_{\sin}[\ell]$ real and independent of δ_{cp}. Additionally, $\hat{\bar{W}}_{\sin}[\ell]$ antisymmetric, whereas $\hat{\bar{W}}_{\cos}[\ell]$ and $\hat{\bar{W}}_0[\ell]$ are symmetric, under exchange of initial and final states. It follows that $\mathrm{Tr}\hat{\bar{W}}_{\cos}[\ell] = \mathrm{Tr}\hat{\bar{W}}_{\sin}[\ell] = 0$ and, therefore,

$$
\mathrm{Tr}\hat{\bar{W}}[\ell] = \mathrm{Tr}\hat{\bar{W}}_0[\ell]. \tag{A10}
$$

Then, from Eq. (A10) and the definition of F_ℓ^{ab} in Eq. (54), we find the trace relationship

$$
\mathrm{Tr}F_\ell = \frac{\mathrm{Tr}\hat{\bar{W}}[\ell]}{\hat{\bar{D}}[\ell]} = 1. \tag{A11}
$$

a. Analytic expressions for $\hat{\bar{W}}_0[\ell]$

For flavor changing transitions, $\nu_i \rightarrow \nu_j$, the matrix elements of $\hat{\bar{W}}_0[\ell]$ are found to have the structure

$$
\begin{aligned}
\langle M(\mu)|\hat{\bar{W}}_0[\ell]|M(e)\rangle &\equiv \hat{\bar{W}}_0^{12}[\ell] = c^{(12)}[\ell] \cos \theta_{23} \\
\langle M(\tau)|\hat{\bar{W}}_0[\ell]|M(e)\rangle &\equiv \hat{\bar{W}}_0^{13}[\ell] = -c^{(12)}[\ell] \sin \theta_{23} \\
\langle M(\tau)|\hat{\bar{W}}_0[\ell]|M(\mu)\rangle &\equiv \hat{\bar{W}}_0^{23}[\ell] = c^{(23)}[\ell] \sin 2\theta_{23}.
\end{aligned} \tag{A12}
$$

We use the convention that a quantity $O^{(ab)}$ written *with* parentheses enclosing ab is a number, not a matrix element. As noted, O^{ab} written *without* parentheses surrounding ab is a matrix element. This distinction may be obvious in the present context, but later on this distinction may not be so obvious.

Note that $\hat{\bar{W}}_0^{e\mu}[\ell]$ and $\hat{\bar{W}}_0^{e\tau}[\ell]$ are not independent. The corresponding coefficients $c^{(ii)}[\ell]$ of for flavor preserving transitions are defined with $\hat{\bar{E}}_\ell^2$ in Eq. (A8) separated out,

$$
\begin{aligned}
\langle M(i)|\hat{\bar{W}}_0[\ell]|M(i)\rangle &\equiv \hat{\bar{W}}_0^{ii}[\ell] \\
&= \hat{\bar{E}}_\ell^2 + c^{(ii)}[\ell].
\end{aligned} \tag{A13}
$$

The matrix for $\hat{\bar{W}}_0[\ell]$ is, thus,

$$\hat{\bar{W}}_0[\ell] = \mathbf{1} \times \hat{\bar{E}}_\ell^2 + \begin{pmatrix} c^{(11)}[\ell] & c^{(12)}[\ell]\cos\theta_{23} & -c^{(12)}[\ell]\sin\theta_{23} \\ c^{(12)}[\ell]\cos\theta_{23} & c^{(22)}[\ell] & c^{(23)}[\ell]\sin 2\theta_{23} \\ -c^{(12)}[\ell]\sin\theta_{23} & c^{(23)}[\ell]\sin 2\theta_{23} & c^{(33)}[\ell] \end{pmatrix}. \tag{A14}$$

Writing the dependence of $c^{(ij)}[\ell]$ on $\hat{\bar{E}}_\ell$ explicitly,

$$c^{(ij)}[\ell] = c_0^{(ij)} + c_1^{(ij)}\hat{\bar{E}}_\ell, \tag{A15}$$

and expressing the results in terms of the combinations of mixing angles,

$$C_1^{(\pm)} \equiv \cos^2\theta_{12}\cos^2\theta_{23} \pm \sin^2\theta_{23}\sin^2\theta_{12}\sin^2\theta_{13}$$
$$C_2^{(\pm)} \equiv \cos^2\theta_{12} \pm \sin^2\theta_{12}\sin^2\theta_{13}, \tag{A16}$$

where $C_2^{(\pm)}$ was defined earlier in Eq. (36), we find the following exact results. For the flavor-changing transitions,

$$c_0^{(12)} = -c_1^{(12)} = -\frac{\alpha}{2}\cos\theta_{13}\sin 2\theta_{12}$$
$$c_0^{(23)} = -\frac{\alpha}{2}(\sin^2\theta_{12} - \cos^2\theta_{12}\sin^2\theta_{13})$$
$$\qquad\quad - \frac{\hat{A}}{2}(\cos^2\theta_{13} - \alpha C_2^{(-)})$$
$$c_1^{(23)} = \frac{1}{2}(\cos^2\theta_{13} - \alpha C_2^{(-)}), \tag{A17}$$

and for the flavor-preserving transitions,

$$c_0^{(11)} = \alpha\cos^2\theta_{12}\cos^2\theta_{13}$$
$$c_1^{(11)} = -\cos^2\theta_{13} - \alpha C_2^{(+)}, \tag{A18}$$

$$c_0^{(22)} = \alpha(1 - \sin^2\theta_{23}\cos^2\theta_{13} - C_2^{(+)})$$
$$\qquad\quad + \hat{A}(\cos^2\theta_{13}\cos^2\theta_{23} + \alpha(C_2^{(+)} - C_1^{(+)}))$$
$$c_1^{(22)} = -1 + \cos^2\theta_{13}\sin^2\theta_{23} - \alpha(1 - C_1^{(+)}) - \hat{A}. \tag{A19}$$

The coefficients $c^{(33)}$ follow from $c^{(22)}$ by the exchange $\sin\theta_{23} \leftrightarrow \cos\theta_{23}$. Consequently, there are only four independent matrix elements for $\hat{\bar{W}}_0[\ell]$, two diagonal and two off-diagonal. With the eigenvalues independent of θ_{23}, it follows that

$$\hat{\bar{W}}_0^{\tau\tau}[\ell] = \hat{\bar{W}}_0^{\mu\mu}[\ell]|_{\sin\theta_{23} \leftrightarrow \cos\theta_{23}}. \tag{A20}$$

b. Analytic expressions for $\hat{\bar{W}}_{\sin}[\ell]$ and $\hat{\bar{W}}_{\cos}[\ell]$

The matrices for $\hat{\bar{W}}_{\sin}[\ell]$ and $\hat{\bar{W}}_{\cos}[\ell]$ have the following simple structure

$$\hat{\bar{W}}_{\sin}[\ell] = \begin{pmatrix} 0 & -a^{(12)}[\ell]\sin\theta_{23} & -a^{(12)}[\ell]\cos\theta_{23} \\ a^{(12)}[\ell]\sin\theta_{23} & 0 & a^{(23)}[\ell] \\ a^{(12)}[\ell]\cos\theta_{23} & -a^{(23)}[\ell] & 0 \end{pmatrix} \tag{A21}$$

and

$$\hat{\bar{W}}_{\cos}[\ell] = \begin{pmatrix} 0 & a^{(12)}[\ell]\sin\theta_{23} & a^{(12)}[\ell]\cos\theta_{23} \\ a^{(12)}[\ell]\sin\theta_{23} & -a^{(23)}[\ell]\sin 2\theta_{23} & -a^{(23)}[\ell]\cos 2\theta_{23} \\ a^{(12)}[\ell]\cos\theta_{23} & -a^{(23)}[\ell]\cos 2\theta_{23} & a^{(23)}[\ell]\sin 2\theta_{23} \end{pmatrix}, \tag{A22}$$

where

$$a^{(23)}[\ell] = a_0^{(23)} + a_1^{(23)}\hat{\bar{E}}_\ell$$
$$a^{(12)}[\ell] = a_0^{(12)} + a_1^{(12)}\hat{\bar{E}}_\ell. \tag{A23}$$

We find the exact results

$$a_0^{(23)} = -\frac{\hat{A}\alpha}{2}\sin 2\theta_{12}\sin\theta_{13} - \frac{\alpha}{2}\sin 2\theta_{12}\sin\theta_{13}$$
$$a_1^{(23)} = \frac{\alpha}{2}\sin 2\theta_{12}\sin\theta_{13}$$
$$a_0^{(12)} = -\frac{\alpha}{2}\cos^2\theta_{12}\sin 2\theta_{13}$$
$$a_1^{(12)} = \frac{1}{2}\sin 2\theta_{13} - \frac{\alpha}{2}\sin^2\theta_{12}\sin 2\theta_{13}. \tag{A24}$$

c. Interconnections among $\hat{\bar{W}}_0[\ell]$, $\hat{\bar{W}}_{\sin}[\ell]$, and $\hat{\bar{W}}_{\cos}[\ell]$

Significant simplifications arise from interconnections among $W_0[\ell]$, $W_{\cos}[\ell]$, and $W_{\sin}[\ell]$. One of these follows from Eqs. (A21) and (A22), which show that the matrix elements of $\hat{\bar{W}}_{\cos}[\ell]$ and $\hat{\bar{W}}_{\sin}[\ell]$ are proportional, namely,

$$\langle M(a)|\hat{\bar{W}}_{\sin}[\ell]|M(b)\rangle = f_{ab}\langle M(a)|\hat{\bar{W}}_{\cos}[\ell]|M(b)\rangle, \quad \text{(A25)}$$

with the constants of proportionality f_{ab} independent of ℓ,

$$f_{ab} = \begin{pmatrix} 0 & -1 & -1 \\ 1 & 0 & -\cos^{-1}2\theta_{23} \\ 1 & \cos^{-1}2\theta_{23} & 0 \end{pmatrix}. \quad \text{(A26)}$$

Another follows from Eqs. (A17) and (A24), from which it follows that

$$a_1^{(12)}c_0^{(12)} - a_0^{(12)}c_1^{(12)} = 2K$$
$$a_1^{(23)}c_0^{(23)} - a_0^{(23)}c_1^{(23)} = -K. \quad \text{(A27)}$$

The quantity K is

$$K = -\frac{\alpha(1-\alpha)}{8}$$
$$\times \cos\theta_{13}\sin 2\theta_{12}\sin 2\theta_{13}. \quad \text{(A28)}$$

3. Expressions for $S(T)$ in terms of δ_{cp}

The dependence of $S(T)$ on the CP violating phase δ_{cp} is very simple and follows from Eqs. (A5) and (A9), noting that $F_\ell^{ab} = \hat{\bar{W}}^{ab}[\ell]/\hat{\bar{D}}[\ell]$, Eq. (56). We, thus, find

$$\mathrm{Re}[S^{ab}(t',t)] = \delta_{ab} - 2\sum_\ell \frac{\hat{\bar{W}}_0^{ab}[\ell]}{\hat{\bar{D}}[\ell]}\sin^2\hat{\bar{E}}_\ell\Delta_L$$
$$- 2\cos\delta_{cp}\sum_\ell \frac{\hat{\bar{W}}_{\cos}^{ab}[\ell]}{\hat{\bar{D}}[\ell]}\sin^2\hat{\bar{E}}_\ell\Delta_L$$
$$+ \sin\delta_{cp}\sum_\ell \frac{\hat{\bar{W}}_{\sin}^{ab}[\ell]}{\hat{\bar{D}}[\ell]}\sin 2\hat{\bar{E}}_\ell\Delta_L, \quad \text{(A29)}$$

and

$$\mathrm{Im}[S^{ab}(t',t)] = -2\sin\delta_{cp}\sum_\ell \frac{\hat{\bar{W}}_{\sin}^{ab}[\ell]}{\hat{\bar{D}}[\ell]}\sin^2\hat{\bar{E}}_\ell\Delta_L$$
$$- \sum_\ell \frac{\hat{\bar{W}}_0^{ab}[\ell]}{\hat{\bar{D}}[\ell]}\sin 2\hat{\bar{E}}_\ell\Delta_L$$
$$- \cos\delta_{cp}\sum_\ell \frac{\hat{\bar{W}}_{\cos}^{ab}[\ell]}{\hat{\bar{D}}[\ell]}\sin 2\hat{\bar{E}}_\ell\Delta_L. \quad \text{(A30)}$$

The dependence of $S(L)$ on $\hat{\bar{E}}_\ell$ and the remaining parameters of H_ν are given analytically through Eqs. (A14), (A21), and (A22).

APPENDIX B: OSCILLATION PROBABILITY $\mathcal{P}(\nu_a \to \nu_b)$ IN OUR HAMILTONIAN FORMULATION

The neutrino oscillation probabilities are obtained directly from our expression for the time-evolution operator, Eq. (106). In the high-energy limit, the oscillation probability in Eq. (71), expressed in terms of $\mathrm{Re}[F_{\ell\ell'}^{ab}]$ and $\mathrm{Im}[F_{\ell\ell'}^{ab}]$, is

$$\mathcal{P}(\nu_a \to \nu_b) = 2\sum_{\ell>\ell'}\mathrm{Im}[F_{\ell\ell'}^{ab}]\sin(2\Delta\hat{\bar{E}}_{\ell\ell'}\Delta_L)$$
$$+ 2\sum_{\ell>\ell'}\mathrm{Re}[F_{\ell\ell'}^{ab}]\cos(2\Delta\hat{\bar{E}}_{\ell\ell'}\Delta_L), \quad \text{(B1)}$$

where $1 \le \ell \le 3$, where Δ_L was defined in Eq. (33), and $\Delta\hat{\bar{E}}_{\ell\ell'}$ in Eq. (43).

Note that $\mathrm{Re}[F_{\ell\ell'}^{ab}]$ satisfies a normalization condition,

$$\sum_{\ell\ell'}\mathrm{Re}F_{\ell\ell'}^{ab} = \delta_{ab}, \quad \text{(B2)}$$

found by evaluating Eq. (71) at $t = t'$ and recognizing that $\mathcal{P}(\nu_a \to \nu_b)$ is a real number. Taking Eq. (B2) into account and using the identity $1 - \cos 2\beta \equiv 2\sin^2\beta$, we find an equivalent expression,

$$\mathcal{P}(\nu_a \to \nu_b) = \delta_{ab} + 2\sum_{\ell>\ell'}\mathrm{Im}[F_{\ell\ell'}^{ab}]$$
$$\times \sin(2\Delta\hat{\bar{E}}_{\ell\ell'}\Delta_L)$$
$$- 4\sum_{\ell>\ell'}\mathrm{Re}F_{\ell\ell'}^{ab}\sin^2(\Delta\hat{\bar{E}}_{\ell\ell'}\Delta_L), \quad \text{(B3)}$$

that bears a striking similarity to the familiar vacuum expression with $F_{\ell\ell'}^{ab}$ playing a role analogous to $J_{\ell\ell'}^{ab}$ (as, for example, in Eq. (1) of Ref. [4]). Equations (B1) and (B3) make use of the fact that a probability is purely real.

1. Properties of $F_{\ell\ell'}^{ab}$

It follows from Eq. (72) and the observation that the energy of a neutrino or antineutrino in matter is independent of δ_{cp} that $F_{\ell\ell'}^{ab}$ is symmetric under the simultaneous exchange of a, b and ℓ, ℓ',

$$F_{\ell\ell'}^{ab} = F_{\ell'\ell}^{ba}. \quad \text{(B4)}$$

Using in addition the Hermiticity of $\hat{\bar{W}}[\ell]$, Eq. (59), we find the reflection symmetry,

$$F_{\ell\ell'}^{ba} = F_{\ell\ell'}^{ab*}$$
$$F_{\ell'\ell}^{ab} = F_{\ell\ell'}^{ab*}. \tag{B5}$$

From this, along with Eq. (B4), it follows that $\mathrm{Im}F_{\ell\ell'}^{ab}$ is antisymmetric under the exchange of either (a,b) or (ℓ,ℓ'),

$$\mathrm{Im}F_{\ell\ell'}^{ab} = -\mathrm{Im}F_{\ell'\ell}^{ab} = -\mathrm{Im}F_{\ell\ell'}^{ba}, \tag{B6}$$

whereas $\mathrm{Re}F_{\ell\ell'}^{ab}$ is symmetric,

$$\mathrm{Re}F_{\ell\ell'}^{ab} = \mathrm{Re}F_{\ell'\ell}^{ab} = \mathrm{Re}F_{\ell\ell'}^{ba}. \tag{B7}$$

There are no symmetries connecting the $F_{\ell\ell'}^{ab}$ of neutrinos to those of antineutrinos because these energies are, in general, different. This is not the case, however, in the vacuum for theories invariant under *CPT*.

2. General expressions for $F_{\ell\ell'}^{ab}$

The quantity $F_{\ell\ell'}^{ab}$ is most easily obtained from $w_{\ell\ell'}^{ab}$,

$$w_{\ell\ell'}^{ab} \equiv \langle M(b)|\hat{\bar{W}}[\ell]|M(a)\rangle$$
$$\times \langle M(b)|\hat{\bar{W}}[\ell']|M(a)\rangle^*. \tag{B8}$$

Analytic formulas for $w_{\ell,\ell'}^{ab}$ are easily obtained in terms of the parameters of H_ν using $\hat{\bar{W}}[\ell]$ given in Eq. (A9). Equation (72) then gives $F_{\ell\ell'}^{ab}$ as

$$F_{\ell\ell'}^{ab} = \frac{w_{\ell\ell'}^{ab}}{\hat{\bar{D}}[\ell]\hat{\bar{D}}[\ell']}. \tag{B9}$$

Because $\hat{\bar{W}}[\ell]$ consists of three terms, one proportional to $\sin\delta_{cp}$, one proportional to $\cos\delta_{cp}$, and one independent of δ_{cp}, the dependence of $w^{ab}[\ell,\ell']$ on δ_{cp} can be expressed *a priori* through the five operators,

$$w_{\ell\ell'}^{ab} = w_{0\ell\ell'}^{ab} + \cos\delta_{cp}w_{\cos\ell\ell'}^{ab}$$
$$+ \cos^2\delta_{cp}w_{\cos^2\ell\ell'}^{ab} + i\Big(\sin\delta_{cp}w_{\sin\ell\ell'}^{ab}$$
$$+ \sin\delta_{cp}\cos\delta_{cp}w_{\sin\times\cos\ell\ell'}^{ab}\Big), \tag{B10}$$

each of which is uniquely determined by Eqs. (A9) and (B8). Clearly, just as for the $\hat{\bar{W}}_i[\ell]$, the matrix elements of $w_i[\ell,\ell']$ are real and independent of δ_{cp}.

Using the Hermiticity of $\hat{\bar{W}}_0[\ell]$ and $\hat{\bar{W}}_{\cos}[\ell]$, and the anti-Hermiticity of $\hat{\bar{W}}_{\sin}[\ell]$, we then find

$$w_{0\ell\ell'}^{ab} \equiv \hat{\bar{W}}_0^{ab}[\ell]\hat{\bar{W}}_0^{ab}[\ell'] + \hat{\bar{W}}_{\sin}^{ab}[\ell]\hat{\bar{W}}_{\sin}^{ab}[\ell']$$

$$w_{\sin\ell\ell'}^{ab} \equiv \hat{\bar{W}}_{\sin}^{ab}[\ell]\hat{\bar{W}}_0^{ab}[\ell'] - \hat{\bar{W}}_0^{ab}[\ell]\hat{\bar{W}}_{\sin}^{ab}[\ell']$$

$$w_{\cos\ell\ell'}^{ab} \equiv \hat{\bar{W}}_{\cos}^{ab}[\ell]\hat{\bar{W}}_0^{ab}[\ell'] + \hat{\bar{W}}_0^{ab}[\ell]\hat{\bar{W}}_{\cos}^{ab}[\ell']$$

$$w_{\cos^2\ell\ell'}^{ab} \equiv \hat{\bar{W}}_{\cos}^{ab}[\ell]\hat{\bar{W}}_{\cos}^{ab}[\ell'] - \hat{\bar{W}}_{\sin}^{ab}[\ell]\hat{\bar{W}}_{\sin}^{ab}[\ell']$$

$$w_{\sin\times\cos\ell\ell'}^{ab} \equiv \hat{\bar{W}}_{\sin}^{ab}[\ell]\hat{\bar{W}}_{\cos}^{ab}[\ell'] - \hat{\bar{W}}_{\cos}^{ab}[\ell]\hat{\bar{W}}_{\sin}^{ab}[\ell']. \tag{B11}$$

Note that Eqs. (A25) and (A26) require that $w_{\sin\times\cos}$ vanish identically,

$$w_{\sin\times\cos}^{ab} = 0, \tag{B12}$$

so this term need not be considered further. Note also that the dependence of $w_{i\ell\ell'}^{ab}$ on ℓ and ℓ' arises entirely from the eigenvalues $\hat{\bar{E}}_\ell$ and $\hat{\bar{E}}_{\ell'}$, as $\hat{\bar{W}}^{ab}[\ell]$ depends on ℓ entirely through $\hat{\bar{E}}_\ell$. Finally, we will find it useful to define $w_i^{ab}[\ell]$ in analogy to $\hat{\bar{W}}[\ell]$ in Eq. (57),

$$w_i^{ab}[1] \equiv w_i^{ab}[3,2]$$
$$w_i^{ab}[2] \equiv w_i^{ab}[3,1]$$
$$w_i^{ab}[3] \equiv w_i^{ab}[2,1]. \tag{B13}$$

These are the only three $w_i^{ab}[\ell,\ell']$ needed because of the restriction $\ell > \ell'$ in Eq. (B3).

3. Analytic expressions for $w_{\sin}^{ab}[\ell,\ell']$

From the symmetries of $\hat{\bar{W}}_0^{ab}[\ell]$, $\hat{\bar{W}}_{\cos}^{ab}[\ell]$, and $\hat{\bar{W}}_{\sin}^{ab}[\ell]$, we see from Eq. (B11) that $w_{\sin\ell\ell'}^{ab}$ is odd under the exchange of either a, b or ℓ, ℓ'. The term $w_{\sin\ell,\ell'}^{ab}$, therefore, vanishes for $a = b$ [and for $\ell = \ell'$], but again recall that restrictions on the sums is such that $w_{\ell\ell'}^{ab}$ contributes only for $\ell > \ell'$.

Using the general results in Eqs. (A14), (A21), and (A22), we find $w_{\sin\ell\ell'}^{ab}$ given in Eq. (B11) is, as a matrix,

$$w_{\sin\ell\ell'} = \frac{1}{2}\sin 2\theta_{23}\begin{pmatrix} 0 & A & -A \\ -A & 0 & B \\ A & -B & 0 \end{pmatrix}, \tag{B14}$$

where

$$A = -(a^{(12)}[\ell]c^{(12)}[\ell'] - c^{(12)}[\ell]a^{(12)}[\ell'])$$
$$= -(a_1^{(12)}c_0^{(12)} - a_0^{(12)}c_1^{(12)})\Delta\hat{\bar{E}}_{\ell\ell'} \tag{B15}$$

and

$$B = 2(a^{(23)}[\ell]c^{(23)}[\ell'] - c^{(23)}[\ell]a^{(23)}[\ell'])$$
$$= 2(a_1^{(23)}c_0^{(23)} - a_0^{(23)}c_1^{(23)})\Delta\hat{\bar{E}}_{\ell\ell'}. \tag{B16}$$

We see from Eq. (A27) that $A = B$, so from Eq. (B14) we find the following simple expression,

$$w_{\sin \ell \ell'}^{ab} = K \sin 2\theta_{23} \Delta \hat{\bar{E}}_{\ell \ell'} \epsilon_{\sin}^{ab}, \tag{B17}$$

and correspondingly

$$w_{\sin}^{ab}[\ell] = K \sin 2\theta_{23} \Delta \hat{\bar{E}}[\ell] \epsilon_{\sin}^{ab}, \tag{B18}$$

where $\epsilon_{\sin}$ is the antisymmetric matrix

$$\epsilon_{\sin} \equiv \begin{pmatrix} 0 & 1 & -1 \\ -1 & 0 & 1 \\ 1 & -1 & 0 \end{pmatrix}. \tag{B19}$$

4. Analytic expressions for $w_{\cos^2}^{ab}$, $w_{\cos}^{ab}$, and w_0^{ab}

We also see from the symmetries of $\hat{\bar{W}}_0^{ab}[\ell]$, $\hat{\bar{W}}_{\cos}^{ab}[\ell]$, and $\hat{\bar{W}}_{\sin}^{ab}[\ell]$, that $w_{0\ell\ell'}^{ab}$, $w_{\cos \ell\ell'}^{ab}$, and $w_{\cos^2 \ell\ell'}^{ab}$ are even under the exchange of a, b and/or ℓ, ℓ'. Since the dependence of all $w_{i\ell\ell'}^{ab}$ on ℓ and ℓ' arises entirely from the eigenvalues $\hat{\bar{E}}_\ell$ and $\hat{\bar{E}}_{\ell'}$, it follows that the terms symmetric in ℓ and ℓ' must be functions of symmetric combinations of $\hat{\bar{E}}_\ell$ and $\hat{\bar{E}}_{\ell'}$.

There are only three irreducible symmetric functions of $\hat{\bar{E}}_\ell$ and $\hat{\bar{E}}_{\ell'}$: a constant, the sum $\hat{\bar{E}}_\ell + \hat{\bar{E}}_{\ell'}$, and the product $\hat{\bar{E}}_\ell \hat{\bar{E}}_{\ell'}$, just as for $\hat{\bar{W}}[\ell]$ in Eq. (A6). Thus, we anticipate that the entire dependence of $w_0^{ab}[\ell]$, $w_{\cos}^{ab}[\ell]$, and $w_{\cos^2}^{ab}[\ell]$ on ℓ will occur through $\Sigma[\ell]$ and $\Pi[\ell]$ in Eqs. (A7) and (A8) and, hence, through $\hat{\bar{E}}_\ell$, as for $\hat{\bar{W}}[\ell]$.

In the following discussion, it is important to recall our convention that a quantity, such as $w^{(ab)}[\ell]$, written *with* parentheses enclosing ab is a number, whereas $w^{ab}[\ell]$ written *without* parentheses surrounding ab is the element of a matrix $w[\ell]$,

$$w^{ab}[\ell] \equiv \langle M(b)|w[\ell]|M(a)\rangle. \tag{B20}$$

a. Matrix elements of $w_{\cos^2}$

Using Eq. (B11) with Eqs. (A21) and (A22), the matrix for $w_{\cos^2}$ is found to be

$$w_{\cos^2} = \sin^2 2\theta_{23} \begin{pmatrix} 0 & 0 & 0 \\ 0 & w_{\cos^2}^{(22)} & -w_{\cos^2}^{(22)} \\ 0 & -w_{\cos^2}^{(22)} & w_{\cos^2}^{(22)} \end{pmatrix}, \tag{B21}$$

where

$$\begin{aligned} w_{\cos^2 \ell\ell'}^{(22)} &= a^{(23)}[\ell]a^{(23)}[\ell'] \\ &= a_0^{(23)2} + a_0^{(23)}a_1^{(23)}(\hat{\bar{E}}_\ell + \hat{\bar{E}}_{\ell'}) + a_1^{(23)2}\hat{\bar{E}}_\ell \hat{\bar{E}}_{\ell'}. \end{aligned} \tag{B22}$$

Correspondingly,

$$w_{\cos^2}^{(22)}[\ell] = a_0^{(23)2} + a_0^{(23)}a_1^{(23)}\Sigma[\ell] + a_1^{(23)2}\Pi[\ell]. \tag{B23}$$

Note the somewhat subtle notational distinction between the *operator* $w_{\cos^2}$ and the *coefficients* $w_{\cos^2}^{(ij)}$ in terms of which it is defined. The latter is indicated by parentheses that surrounding the superscripts. By contrast, superscripts without parentheses, as in w_i^{ab}, indicate the transition $\nu_a \rightarrow \nu_b$, i.e., $w_i^{ab} \equiv \langle M(b)|w_i|M(a)\rangle$.

b. Matrix elements of $w_{\cos}$

We find only three independent, nonvanishing matrix elements for $w_{\cos}$, one diagonal element and two off-diagonal elements. As a matrix,

$$w_{\cos} = \sin 2\theta_{23} \begin{pmatrix} 0 & w_{\cos}^{(12)} & -w_{\cos}^{(12)} \\ w_{\cos}^{(12)} & w_{\cos}^{(22)} & w_{\cos}^{(23)} \\ -w_{\cos}^{(12)} & w_{\cos}^{(23)} & w_{\cos}^{(33)} \end{pmatrix}. \tag{B24}$$

The two independent off-diagonal elements,

$$\begin{aligned} w_{\cos \ell\ell'}^{(12)} &= \frac{1}{2}(a^{(12)}[\ell]c^{(12)}[\ell'] + c^{(12)}[\ell]a^{(12)}[\ell']) \\ w_{\cos \ell\ell'}^{(23)} &= -(a^{(23)}[\ell]c^{(23)}[\ell'] + c^{(23)}[\ell]a^{(23)}[\ell']) \cos 2\theta_{23}, \end{aligned} \tag{B25}$$

follow immediately from the structure of $\hat{\bar{W}}_0^{ab}[\ell']$ and $\hat{\bar{W}}_{\cos}^{ab}[\ell]$ given in Eqs. (A14) and (A22), respectively.

Taking $w_{\cos}^{(22)}$ from Eqs. (A14), (A22), and (B11), we obtain

$$\begin{aligned} w_{\cos \ell\ell'}^{(22)} &= -a^{(23)}[\ell](\hat{\bar{E}}_{\ell'}^2 + c^{(22)}[\ell']) \\ &\quad - (\hat{\bar{E}}_\ell^2 + c^{(22)}[\ell])a^{(23)}[\ell']. \end{aligned} \tag{B26}$$

Similarly, for the diagonal matrix element D,

$$\begin{aligned} w_{\cos \ell\ell'}^{(33)} &= a^{(23)}[\ell](\hat{\bar{E}}_{\ell'}^2 + c^{(33)}[\ell']) \\ &\quad + (\hat{\bar{E}}_\ell^2 + c^{(33)}[\ell])a^{(23)}[\ell']. \end{aligned} \tag{B27}$$

The element $w_{\cos \ell\ell'}^{(11)}$ vanishes as a consequence of $\hat{\bar{W}}_{\cos}^{(11)}[\ell] = 0$.

Correspondingly, for the off-diagonal matrix elements we find

$$w_{\cos}^{(12)}[\ell] = a_0^{(12)}c_0^{(12)} + \frac{1}{2}(a_1^{(12)}c_0^{(12)} + a_0^{(12)}c_1^{(12)})$$
$$\times \Sigma[\ell] + a_1^{(12)}c_1^{(12)}\Pi[\ell]$$

$$w_{\cos}^{(23)}[\ell] = -2\cos 2\theta_{23}a_0^{(23)}c_0^{(23)}$$
$$- \cos 2\theta_{23}(a_1^{(23)}c_0^{(23)} + a_0^{(23)}c_1^{(23)})$$
$$\times \Sigma[\ell] - 2\cos 2\theta_{23}a_1^{(23)}c_1^{(23)}\Pi[\ell], \quad (B28)$$

which simplify somewhat by using Eqs. (A27) and (A28). For the diagonal matrix elements,

$$w_{\cos}^{(22)}[\ell] = -2a_0^{(23)}c_0^{(22)} - (a_1^{(23)}c_0^{(22)} + a_0^{(23)}c_1^{(22)})$$
$$\times \Sigma[\ell] + 2(a_0^{(23)} - a_1^{(23)}c_1^{(22)})\Pi[\ell]$$
$$- a_1^{(23)}\Sigma[\ell]\Pi[\ell] - a_0^{(23)}\Sigma[\ell]^2 \quad (B29)$$

and

$$w_{\cos}^{(33)}[\ell] = 2a_0^{(23)}c_0^{(33)} + (a_1^{(23)}c_0^{(33)} + a_0^{(23)}c_1^{(33)})$$
$$\times \Sigma[\ell] - 2(a_0^{(23)} - a_1^{(23)}c_1^{(33)})\Pi[\ell]$$
$$+ a_1^{(23)}\Sigma[\ell]\Pi[\ell] + a_0^{(23)}\Sigma[\ell]^2. \quad (B30)$$

The matrix elements $w_{\cos}^{(22)}[\ell]$ and $w_{\cos}^{(33)}[\ell]$ are not independent. The reason is that $w_{\cos}^{(33)}[\ell]$ may be found from $w_{\cos}^{(22)}[\ell]$ by making the replacement $\sin\theta_{23} \leftrightarrow \cos\theta_{23}$ [Eq. (A20)] and by flipping the overall sign. Recall that under this replacement, $c^{(22)} \leftrightarrow c^{(33)}$ and that $a^{(23)}$ is independent of $\sin\theta_{23}$.

c. Matrix elements of w_0

We find four independent, nonvanishing matrix elements for w_0, two diagonal and two off-diagonal elements. As a matrix,

$$w_0 = \begin{pmatrix} w_0^{(11)} & w_0^{(12)} & w_0^{(13)} \\ w_0^{(12)} & w_0^{(22)} & w_0^{(23)} \\ w_0^{(13)} & w_0^{(23)} & w_0^{(33)} \end{pmatrix}. \quad (B31)$$

The off-diagonal elements,

$$w_{0\ell\ell'}^{(12)} = c^{(12)}[\ell]c^{(12)}[\ell']\cos^2\theta_{23}$$
$$+ a^{(12)}[\ell]a^{(12)}[\ell']\sin^2\theta_{23}$$
$$w_{0\ell\ell'}^{(13)} = c^{(12)}[\ell]c^{(12)}[\ell']\sin^2\theta_{23}$$
$$+ a^{(12)}[\ell]a^{(12)}[\ell']\cos^2\theta_{23}$$
$$w_{0\ell\ell'}^{(23)} = c^{(23)}[\ell]c^{(23)}[\ell']\sin^2 2\theta_{23}$$
$$+ a^{(23)}[\ell]a^{(23)}[\ell'], \quad (B32)$$

follow immediately from the structure of $\hat{\tilde{W}}_0^{ab}[\ell']$ and $\hat{\tilde{W}}_{\sin}^{ab}[\ell]$ given in Eqs. (A14) and (A21), respectively. The diagonal elements $w_0^{(nn)}$ are found from Eqs. (A14) and (B11),

$$w_{0\ell\ell'}^{(nn)} = (\hat{\tilde{E}}_\ell^2 + c^{(nn)}[\ell])(\hat{\tilde{E}}_{\ell'}^2 + c^{(nn)}[\ell']). \quad (B33)$$

Correspondingly, for the off-diagonal matrix elements,

$$w_0^{(12)}[\ell] = c_0^{(12)2}\cos^2\theta_{23} + a_0^{(12)2}\sin^2\theta_{23}$$
$$+ (c_0^{(12)}c_1^{(12)}\cos^2\theta_{23} + a_0^{(12)}a_1^{(12)}\sin^2\theta_{23})\Sigma[\ell]$$
$$+ (c_1^{(12)2}\cos^2\theta_{23} + a_1^{(12)2}\sin^2\theta_{23})\Pi[\ell]$$

$$w_0^{(13)}[\ell] = c_0^{(12)2}\sin^2\theta_{23} + a_0^{(12)2}\cos^2\theta_{23}$$
$$+ (c_0^{(12)}c_1^{(12)}\sin^2\theta_{23} + a_0^{(12)}a_1^{(12)}\cos^2\theta_{23})\Sigma[\ell]$$
$$+ (c_1^{(12)2}\sin^2\theta_{23} + a_1^{(12)2}\cos^2\theta_{23})\Pi[\ell]$$

$$w_0^{(23)}[\ell] = c_0^{(23)2}\sin^2 2\theta_{23} + a_0^{(23)2}$$
$$+ (a_0^{(23)}a_1^{(23)} + c_0^{(23)}c_1^{(23)}\sin^2 2\theta_{23})\Sigma[\ell]$$
$$+ (c_1^{(23)2}\sin^2\theta_{23} + a_1^{(23)2})\Pi[\ell]. \quad (B34)$$

For the diagonal matrix elements,

$$w_0^{(nn)}[\ell] = c_0^{(nn)2} - (2c_0^{(nn)} - c_1^{(nn)2})\Pi[\ell]$$
$$+ c_0^{(nn)}c_1^{(nn)}\Sigma[\ell] + c_1^{(nn)}\Sigma[\ell]\Pi[\ell]$$
$$+ \Pi[\ell]^2. \quad (B35)$$

As for $w_{\cos}$, the matrix elements $w_0^{(22)}[\ell]$ and $w_0^{(33)}[\ell]$ are not independent. The same is true for $w_0^{(13)}[\ell]$ and $w_0^{(12)}[\ell]$. In both cases the matrix elements may be found from one another by making the replacement $\sin\theta_{23} \leftrightarrow \cos\theta_{23}$ [Eq. (A20)]. Recall that under such a replacement $c^{(22)} \leftrightarrow c^{(33)}$ and that $c^{(12)}$ and $a^{(23)}$ are independent of $\sin\theta_{23}$.

Writing the dependence of the coefficients $w_i^{(mn)}[\ell]$ on $\hat{\tilde{E}}_\ell$ explicitly,

$$w_i^{(mn)}[\ell] = w_{i;0}^{(mn)} + w_{i;1}^{(mn)}\hat{\tilde{E}}_\ell + w_{i;2}^{(mn)}\hat{\tilde{E}}_\ell^2. \quad (B36)$$

5. Analytic expression for $\mathbf{Im}[F_{\ell\ell'}^{ab}]$ and $\mathbf{Re}[F_{\ell\ell'}^{ab}]$

A general form for the real and imaginary parts of $F_{\ell\ell'}^{ab}$ in terms of the four operators, $(w_0, w_{\sin}, w_{\cos}, w_{\cos^2})$ is found from Eq. (72) and Eq. (B10). For $\mathrm{Im}[F_{\ell\ell'}^{ab}]$, using Eq. (B17), we find

$$\mathrm{Im}[F_{\ell\ell'}^{ab}] = \sin\delta_{cp}\frac{w_{\sin\ell\ell'}^{ab}}{\hat{\tilde{D}}[\ell]\hat{\tilde{D}}[\ell']}$$
$$= \frac{1}{2}\sin\delta_{cp}\sin 2\theta_{23}K\epsilon_{\sin}^{ab}\frac{\Delta\hat{\tilde{E}}_{\ell\ell'}}{\hat{\tilde{D}}[\ell]\hat{\tilde{D}}[\ell']}. \quad (B37)$$

Then, using the easily verified result,

$$\frac{\Delta\hat{\bar{E}}_{\ell\ell'}}{\hat{\bar{D}}[\ell]\hat{\bar{D}}[\ell']} = \frac{\epsilon_{\sin}^{\ell\ell'}}{\hat{\bar{D}}}, \qquad (B38)$$

we find

$$\mathrm{Im}F_{\ell\ell'}^{ab} = -\sin\delta_{cp}\epsilon_{\sin}^{ab}\epsilon_{\sin}^{\ell\ell'}\frac{\alpha(1-\alpha)}{8\hat{\bar{D}}}\cos\theta_{13}$$
$$\times \sin 2\theta_{12}\sin 2\theta_{13}\sin 2\theta_{23}. \qquad (B39)$$

For $\mathrm{Re}[F_{\ell\ell'}^{ab}]$ we find

$$\mathrm{Re}[F_{\ell\ell'}^{ab}] = \frac{w_{0\ell\ell'}^{ab}}{\hat{\bar{D}}[\ell]\hat{\bar{D}}[\ell']} + \cos\delta_{cp}\frac{w_{\cos\ell\ell'}^{ab}}{\hat{\bar{D}}[\ell]\hat{\bar{D}}[\ell']}$$
$$+ \cos^2\delta_{cp}\frac{w_{\cos^2\ell\ell'}^{ab}}{\hat{\bar{D}}[\ell]\hat{\bar{D}}[\ell']}. \qquad (B40)$$

Equations (56) and (B38) show that $F_{\ell\ell'}^{ab}$ plays a role for $\mathcal{P}(\nu_a \to \nu_b)$ similar to the one that F_{ℓ}^{ab} plays for $S(T)$. Using Eq. (B10), it follows from Eqs. (B37) and (B40) that $\mathrm{Im}F_{\ell\ell'}^{ab}$ is odd, and $\mathrm{Re}F_{\ell\ell'}^{ab}$, even, under $\delta_{cp} \to -\delta_{cp}$.

[1] L. Wolfenstein, Phys. Rev. D **17**, 2369 (1978).
[2] The ISS Working Group, arXiv:0710.4947.
[3] V. Barger, K. Whisnant, S. Pakvasa, and R. J. N. Phillips, Phys. Rev. D **22**, 2718 (1980).
[4] M. Freund, Phys. Rev. D **64**, 053003 (2001).
[5] E. Akhmedov, P. Huber, M. Lindner, and T. Ohlsson, Nucl. Phys. **B608**, 394 (2001).
[6] M. Jacobson and T. Ohlsson, Phys. Rev. D **69**, 013003 (2004).
[7] E. M. Henley, M. B. Johnson, and L. S. Kisslinger, Int. J. Mod. Phys. E **20**, 2463 (2011).
[8] L. S. Kisslinger, E. M. Henley, and M. B. Johnson, arXiv:1105.2741.
[9] L. S. Kisslinger, E. M. Henley, and M. B. Johnson, Int. J. Mod. Phys. E **21**, 12920(E) (2012).
[10] L. S. Kisslinger, E. M. Henley, and M. B. Johnson, Int. J. Mod. Phys. E **21**, 1250065 (2012).
[11] L. S. Kisslinger, Mod. Phys. Lett. A **30**, 1550014 (2015).
[12] C. W. Kim and W. K. Sze, Phys. Rev. D **35**, 1404 (1987).
[13] H. Davoudiasl, H. S. Lee, and W. J. Marciano, Phys. Rev. D **84**, 013009 (2011).
[14] M. C. Gonzalez-Garcia, M. Maltoni, and J. Salvado, J. High Energy Phys. 05 (2011) 075.
[15] F. P. An *et al.* (Daya Bay Collaboration), Chin. Phys. C **37**, 01101 (2013).
[16] A. Cervera, A. Donini, M. B. Gavela, J. J. Gomez Cádenas, P. Hernández, O. Mena, and S. Rigolin, Nucl. Phys. **B579**, 17 (2000).
[17] M. B. Johnson, E. M. Henley, and L. S. Kisslinger (to be published).
[18] M. B. Johnson, E. M. Henley, and L. S. Kisslinger (to be published).
[19] T. Ohlsson and H. Snellman, Phys. Lett. B **474**, 153 (2000).